

Contents lists available at ScienceDirect

Quaternary Science Reviews

journal homepage: www.elsevier.com/locate/quascirev



Central Equatorial Pacific benthic foraminifera during the mid-Brunhes dissolution interval: Ballasting of particulate organic matter by biogenic silica and carbonate



Hiroyuki Takata ^a, Hyung Jeek Kim ^b, Hirofumi Asahi ^c, Ellen Thomas ^{d, e}, Chan Min Yoo ^b, Sang Bum Chi ^b, Boo-Keun Khim ^{f, *}

- ^a Marine Research Institute, Pusan National University, Busan, 46241, Republic of Korea
- ^b Deep-sea and Seabed Resources Research Division, Korea Institute of Ocean Science and Technology, Busan, 49111, Republic of Korea
- ^c Center for Advanced Marine Core Research, Kochi University, Nankoku, 783-8502, Japan
- ^d Department of Geology and Geophysics, Yale University, New Haven, CT, 06520, USA
- ^e Earth and Environmental Sciences, Wesleyan University, Middletown, CT, 06459, USA
- f Department of Oceanography, Pusan National University, Busan, 46241, Republic of Korea

ARTICLE INFO

Article history: Received 19 December 2018 Received in revised form 18 February 2019 Accepted 25 February 2019 Available online 12 March 2019

Keywords: Quaternary Paleoceanography Equatorial Pacific Biotic response Benthic foraminifera

ABSTRACT

We evaluated the response of Quaternary abyssal benthic foraminifera in cores PC5101 (2°00.86′N, 131°34.32′W) and PC5103 (6°00.10′N, 131°28.57′W) of the Central Equatorial Pacific Ocean to the environmental changes over the past ~520 kyrs, focusing on the mid-Brunhes dissolution interval (~533—191 ka). We used multi-dimensional scaling (MDS) to derive MDS axis 1, reflecting food supply from low (negative scores) to high (positive scores) amounts, and MDS axis 2, reflecting variability in the food supply. From ~120 ka on, *Epistominella exigua*, an indicator of variable food supply, was more abundant in core PC5103 (~6°N) than in core PC5101 (~2°N), but this was reversed from ~300 to 250 ka.

In core PC5101, MDS axis 1 scores are negatively correlated to the biogenic opal mass accumulation rates (MAR) after 249.6 ka, i.e., lower food supply at higher opal-MAR. In contrast, MDS axis 1 scores are positively correlated to the CaCO₃-MAR from 520.8 to 331.2 ka. Both carbonate and opal skeletons might ballast particulate organic matter (POM) to enhance food supply to the benthos, but our data indicate that carbonate is more efficient and that changes in dominant ballasting of POM by different biominerals thus may have significantly affected the biological pump. During the transitional period (~327.5–257.1 ka), ballasting of POM changed from control by calcareous plankton to control by siliceous plankton, with a transient period during which the latitudinal pattern of the Intertropical Convergence Zone was opposite to its modern pattern, with the more variable food supply at ~6°N.

© 2019 Elsevier Ltd. All rights reserved.

1. Introduction

1.1. Oceanographic setting of the equatorial Pacific Ocean

The tropical Pacific Ocean plays an important role in global climate. The Western Pacific Warm Pool (in the Western Equatorial Pacific, WEP) strongly regulates global climate and climate variability through the El Niño-Southern Oscillation (ENSO) (e.g., Meyers et al., 1986; Messie and Chavez, 2013). Upwelling is an important factor in maintaining regional high primary production

* Corresponding author. E-mail address: bkkhim@pusan.ac.kr (B.-K. Khim). in the Eastern Equatorial Pacific (EEP) (e.g., Chavez and Barber, 1987; Messie and Chavez, 2013). Despite its high productivity, the EEP is the largest oceanic source of CO₂ into the atmosphere, emitting about 0.48 Pg-C y⁻¹ through upwelling of cold, deep CO₂-rich waters (Takahashi et al., 2009). The area where cold waters outcrop at the surface, most pronouncedly during La Niña years, has been named the 'cold tongue' (e.g., Jin, 1996). The boundaries of the cold tongue are characterized by the occurrence of tropical instability waves (TIW), short-term perturbations in Sea Surface Temperature (SST) combined with perturbations in productivity (e.g., Legeckis et al., 2004; Willett et al., 2006).

The Intertropical Convergence Zone (ITCZ) is the area close to the equator where the northeast and southeast trade winds converge. Today, in the EEP the ITCZ is located near the equator in boreal winter and spring, and then moves northward in summer and fall (e.g., Amador et al., 2006), oscillating between about 4°N and 11°N (Waliser and Gautier, 1993) (Fig. 1). Monthly chlorophyll-a concentrations in the surface waters along ~131°W (Acker and Leptoukh, 2007) show more frequent seasonal variations between ~6° and ~9°N than between ~0° and ~4°N, which is consistent with seasonal motion of the trade winds (e.g., Fig. 2, Takata et al. (2016)).

In the equatorial high productivity zone, the production of biogenic carbonate (calcareous nannoplankton and planktic foraminifera) and opal (diatoms and radiolarians) in the surface waters is high, and their skeletons as well as organic matter are, in part, exported to the seafloor, resulting in a deeper position of the calcium carbonate compensation depth (CCD) than in other Pacific regions (Theyer et al., 1985; Honjo et al., 1995; Lyle, 2003; Lyle et al., 2008).

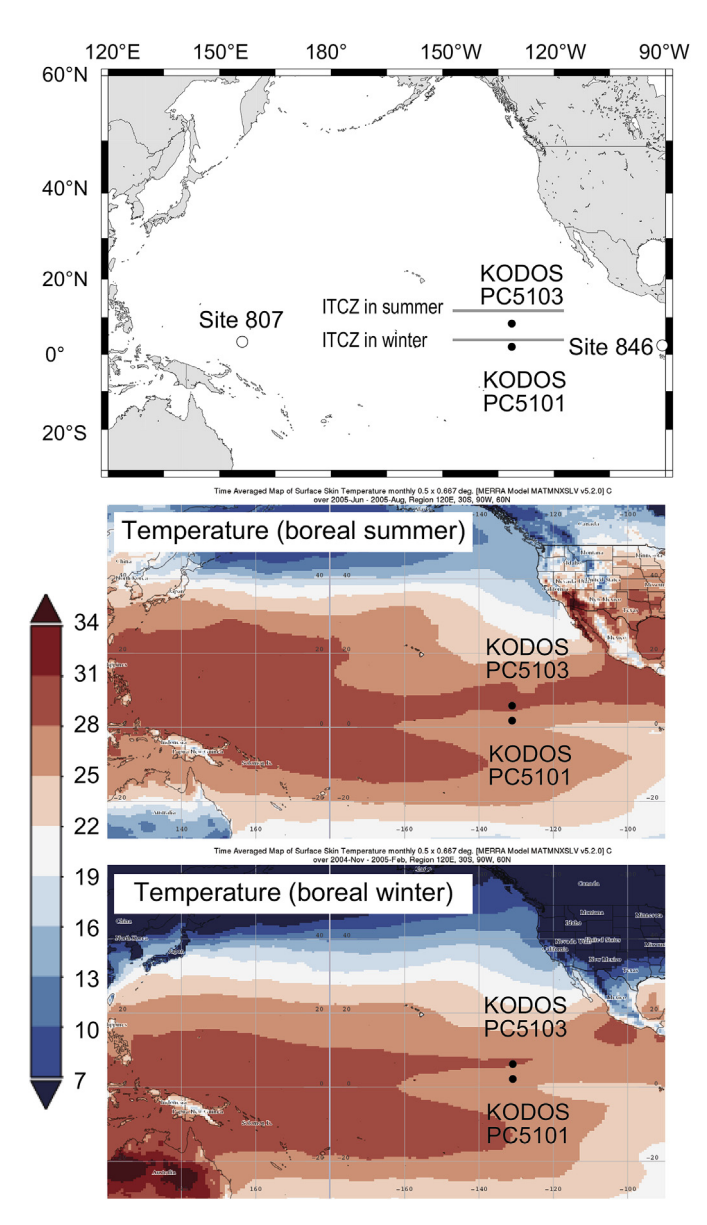


Fig. 1. The location of cores PC5101 and PC5103 in this study and ODP Sites 807 and 846. Surface temperatures of boreal summer (July–September 2005) and winter (December 2004–February 2005) were taken from Acker and Leptoukh (2007).

1.2. Quaternary paleoceanography of the equatorial Pacific Ocean

Carbonate sedimentation in the Equatorial Pacific was enhanced during Plio-Pleistocene glacial periods and reduced during interglacial periods (e.g., Chuey et al., 1987; Farrell and Prell, 1989, 1991; Khim et al., 2012, 2015). Changes in terrigenous and biogenic magnetic mineral sediment fraction coincided with changes in biogenic production at IODP Site U1337 (EEP) (Yamazaki, 2012). The distinct gradient in SST between EEP and WEP as observed today (e.g., via satellite images, Acker and Leptoukh, 2007) is seen in highresolution SST reconstructions for the late Quaternary (De Garidel-Thoron et al., 2005; Horikawa et al., 2010), and may have stabilized since the Mid-Pleistocene Transition (MPT: ~1250-700 ka) (De Garidel-Thoron et al., 2005; Clark et al., 2006; Horikawa et al., 2010). Long-term SST trends during the earlier Quaternary, however, may have differed between EEP and WEP, with a more pronounced decrease in SST in the EEP than in the WEP (e.g., De Garidel-Thoron et al., 2005), mainly due to increased intensity of equatorial upwelling in the EEP.

Surface water characteristics of the Equatorial Pacific Ocean may have changed during the Quaternary, specifically by changes in the intensity of equatorial upwelling with alternation of La Niña-like and El Niño-like conditions (e.g., Zhang et al., 2007; Pena et al., 2008). Planktic foraminiferal and calcareous nannoplankton data indicate that the depth of the thermocline in the WEP (Ocean Drilling Program [ODP] Site 807) may have increased after ~280 ka (MIS 8) (Zhang et al., 2007). Asymmetric seasonal insolation during low precession periods has been argued to have led to the development of persistent La Niña-like conditions in the EEP and enhanced east-west SST gradients, as well as teleconnections between the EEP and the Southern Ocean (Pena et al., 2008). The relative abundance of warm-water calcareous nannoplankton species (indicative of the intensity of the equatorial upwelling) and of upper/lower photic zone taxa (indicative of the depth of nutricline) in the EEP varied over the past ~563 kyrs (Chiyonobu et al., 2006; Chiyonobu, 2009). Earlier times (MIS 14 to MIS 8, ~563-243 ka) were characterized by intense upwelling (La Niñalike condition), whereas the interval from MIS 7 to MIS 1 (243 ka-today) was characterized by weak upwelling (El Niño-like conditions). The biogenic opal content of bulk sediment at ~131°W (Central Equatorial Pacific; CEP), increased during interglacial periods after ~350 ka, as compared to ~164°E (WEP) (Khim et al., 2012).

In addition, significant oceanographic changes occurred in the Equatorial Pacific Ocean during MIS 8 and MIS 7 (~300—191 ka), the later part of the mid-Brunhes dissolution interval (MBDI) (Farrrell and Prell, 1989, 1991; Barker et al., 2006). This interval (MIS 13 to MIS 7; 533—191 ka, centered on MIS 11; 424—374 ka) is characterized by a shallower CCD than that of the present day and earlier times (prior to MIS 14).

At ~300—250 ka, the ITCZ may have been in a different position than it is today (Rea, 1994), with a southward ITCZ displacement proposed to explain the paleoceanographic changes in calcareous nannoplankton (Chiyonobu, 2009) and terrigenous/biogenic magnetic mineral fractions (Yamazaki, 2012). In contrast, McGee et al. (2007) argued that the variability (seasonal-to millennium-scale) of the ITCZ location increased during the last (and possibly earlier) glacial period, but without a significant mean displacement.

In summary, the succession of paleoceanographic changes in the Equatorial Pacific during MIS 8 and MIS 7 (300—191 ka) is still little understood, especially in the CEP. Specifically, there is no agreement on the timing of ITCZ displacement: e.g., during MIS 8/7 (Chiyonobu, 2009), or after MIS 8 (Yamazaki, 2012). New data about deep-sea environments over that time interval thus may provide important clues to the paleoceanographic history in that region

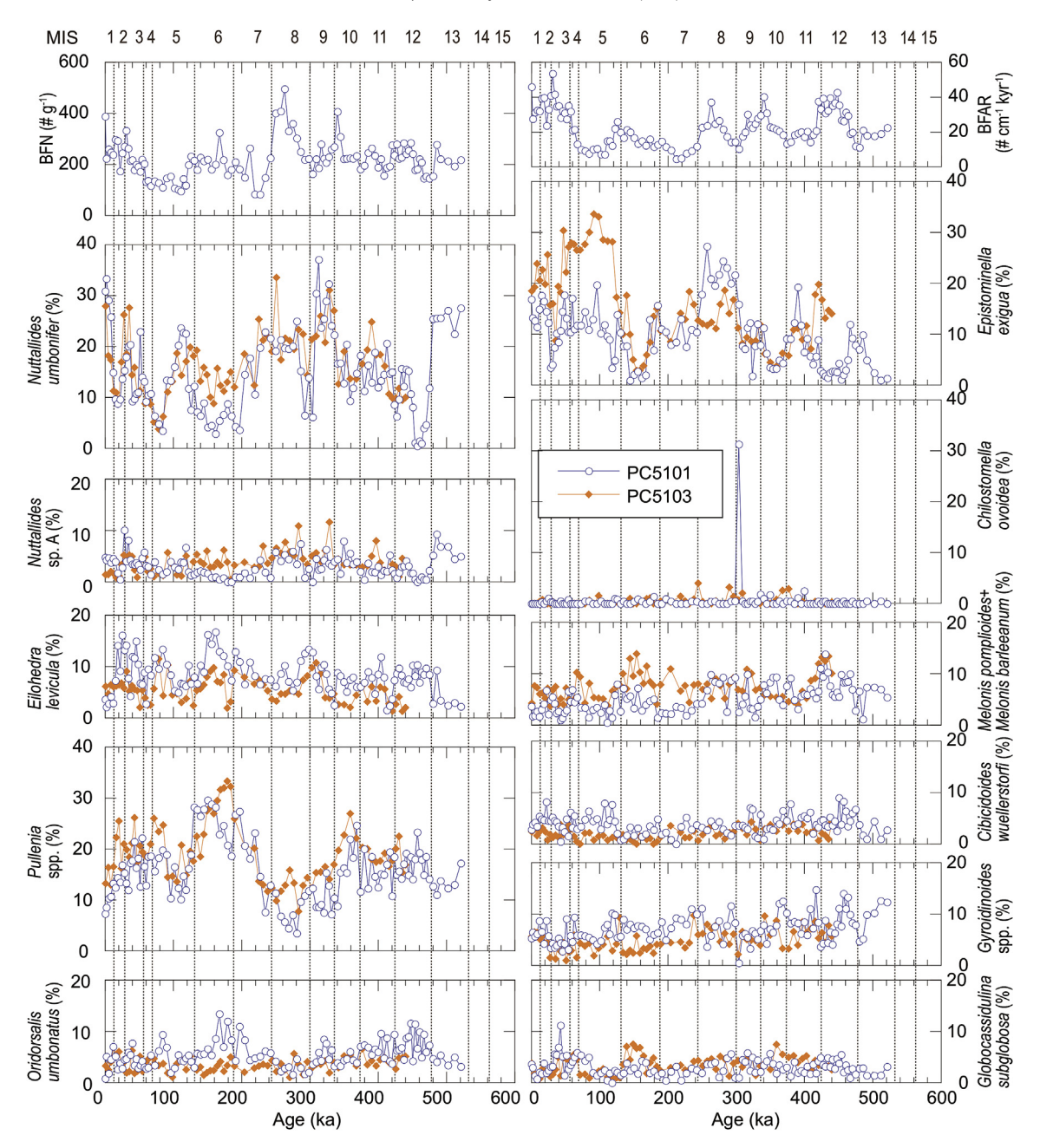


Fig. 2. Stratigraphic changes of the Benthic Foraminiferal Number (BFN), Benthic Foraminiferal Accumulation Rate (BFAR), and relative abundances of the eleven most common taxa of benthic foraminifera (including 53 data points from Takata et al., [2011] and 41 data points from Takata et al. (2016)) of cores PC5101 and PC5103.

(e.g., the Walker Circulation and the position of the ITCZ).

1.3. Our approach: faunal analysis of deep-sea benthic foraminifera

Marine biota, such as planktic and neritic benthic organisms, are sensitive to environmental change (e.g., Yasuhara and Cronin, 2008; Yasuhara et al., 2008, 2009, 2012), so we can evaluate long-term changes in biodiversity of the deep-sea, the largest habitat on Earth, based on microfossil data (e.g., Yasuhara et al., 2017). Only a very small fraction (~1% or less) of the organic matter produced in the photic zone of the Equatorial Pacific reaches the deep-sea floor, because the particle export efficiency (i.e., the proportion of primary production that is exported from the surface ocean) is very low due to extensive remineralization in the upper ocean (Henson et al., 2012). The fraction of organic matter settling down to the

seafloor may well have changed over time, because it depends strongly on ecosystem structure in the upper ocean (Boyd and Trull, 2007; Henson et al., 2012), which changes with seawater temperature and nutrient supply from subsurface waters (e.g., López-Urrutia et al., 2006; O'Connor et al., 2009).

Benthic foraminifera provide information on past trophic conditions, particularly on the total amount and variability of the food supply to the seafloor (e.g., Ohkushi et al., 2000; Gooday, 2003; Smart et al., 2007; Jorissen et al., 2007). In the Equatorial Pacific, we expect to see the effects of changes in the position of the ITCZ and location and intensity of TIWs on productivity and its variability. Enhanced variability of the food supply from the surface ocean (i.e., variability due to seasonal, TIW or ENSO effects) affected benthic foraminifera in the CEP intermittently from MIS 1 to late MIS 5 (~last 110 ka) (Takata et al., 2011).

Here, we quantitatively examine the benthic foraminiferal assemblages over the last ~520 ka in sediment cores PC5101 and PC5103, collected at ~2°N and 6°N, respectively, along ~131°W in the EEP, in order to describe the faunal composition of benthic foraminifera. We compare the faunal data with records of CaCO₃ and biogenic opal contents, aiming to evaluate the benthic foraminiferal response to paleoceanographic changes, particularly from early MIS 5 to MIS 7 (~75–243 ka) (Takata et al., 2011). In addition, we consider differences in benthic assemblages between ~2°N and ~6°N during MIS 8 to MIS 7 (~300–191 ka), especially in terms of the position of the ITCZ along ~131°W.

2. Materials and methods

2.1. Study materials

Our study area is located in the westernmost extension of the 'cold tongue' in the EEP (e.g., http://oceanmotion.org/html/impact/el-nino.htm) (Fig. 1). Piston cores PC5101 (547 cm) and PC5103 (671 cm long) were collected at ~2N (2°00.86′N, 131°34.32′W; 4425 m water depth) and ~6N (6°00.10′N, 131°28.57′W; 4095 m water depth), respectively, on the 2005 R/V *Onnuri* cruise (KODOS05-1) (Fig. 1). Core PC5103 is situated at the southern margin of the modern ITCZ during the boreal winter. Sediments of both cores consist dominantly of white calcareous nannofossil ooze. The total organic carbon content of bulk sediments in core PC5101 is less than 1.2% (Khim et al., 2012), and its biogenic CaCO₃ and opal content show distinctly cyclic glacial and interglacial changes (Khim et al., 2012, 2015).

2.2. Analytical methods

2.2.1. Age models for cores PC5101 and PC5103

We obtained the age model by correlating CaCO $_3$ content of core PC5101 to that of core RC11-210 (Khim et al., 2012), then refined it by measuring oxygen isotope values of the benthic foraminifer *Cibicidoides wuellerstorfi* (>250 µm fraction) from 457 to 0 cm, at 4-cm intervals (137 samples). We used an automated carbonate preparation device (Carousel-48) coupled to a gas-ratio mass spectrometer (Finnigan MAT 251) at the University of Michigan. Crushed samples were reacted with dehydrated phosphoric acid under vacuum at 70 °C. The isotope ratios were calibrated based on the repeated measurements of NBS-19; the analytical precision (1 σ) is \pm 0.05%. For core PC5103, we used the oxygen isotope values of the planktic foraminifera *Globigerinoides sacculifer* (Khim et al., 2015).

Orbitally-tuned age models for cores PC5101 and PC5103 were based upon the combination of oxygen isotopes (PC5101: benthic foraminifera *C. wuellerstorfi*; PC5013: planktic foraminifera *G. sacculifer*), combined with the published CaCO₃ stratigraphy (Khim et al., 2012, 2015) (Supplements 1 and 2). The stratigraphic correlation of both cores with the reference data (LR04: Lisecki and Raymo, 2005; RC11-210: Chuey et al., 1987) was performed using the dynamic matching program "Match 2.3" (Lisecki and Lisecki, 2002). All oxygen isotope data were normalized prior to the matching procedure.

In the Equatorial Pacific, the major contrast in CaCO₃ (weight %) on glacial—interglacial timescales is a powerful tool in establishing an orbitally—tuned age model (e.g. Farrell and Prell, 1989; Thomas et al., 2000; Khim et al., 2012, 2015). At core PC5103, several planktic foraminiferal oxygen isotope peaks were excluded from the stratigraphic correlation because they did not agree with CaCO₃ stratigraphy (Khim et al., 2012, 2015: Chapter 3.1). The bottom ages of the cores were assigned to be 621 ka (transition between MIS 16 and MIS 15) for core PC5101, and 922 ka (glacial maxima in MIS 24)

for core PC5103, using the age—depth correlations initially made using CaCO₃ contents (Khim et al., 2012, 2015).

2.2.2. Faunal analysis

Sediment was sliced at 1-cm interval and freeze-dried. For the benthic foraminiferal analysis of core PC5101, one to two grams of sediment were used from 457 to 0 cm at 4-cm intervals. These samples were soaked in warm water and wet-sieved using a 63 umsieve. More than 200 benthic foraminiferal specimens were picked, identified, and counted in the $>105 \, \mu m$ fraction from 457 to 212 cm (59 samples), using a binocular microscope. Taxonomic assignments followed Van Morkhoven et al. (1986) and Jones (1994), with the generic classification of Loeblich and Tappan (1987). We conducted similar analysis on samples from core PC5103 from 301 to 164 cm (35 samples) at 4-cm intervals. We combined these data with those for the upper 209 cm of core PC5101 (53 samples) and for the upper 161 cm interval of core PC5103 (41 samples) (Takata et al., 2011, 2016). The Benthic Foraminiferal Accumulation Rate (BFAR; Herguera and Berger, 1991) was calculated as follows: BFAR $(\# \text{ cm}^{-2} \text{ ky}^{-1}) = \text{BF * LSR * DBD}$, where BF is the number of benthic foraminifera per gram of bulk sediment, LSR is the linear sedimentation rate (cm ky^{-1}), and DBD is the dry bulk density (g cm⁻³) of the sediment.

2.2.3. Perfect test ratio of Globorotalia menardii

We analyzed the perfect test ratio of *Globorotalia menardii* to evaluate the degree of carbonate dissolution on the seafloor, following Kimoto et al. (2003). *Globorotalia menardii* specimens were picked from the >250 μ m fraction of cores PC5101 and PC5103 at 8-cm intervals. According to completeness of the test, "perfect" and "imperfect" specimens were distinguished and counted. We could evaluate the perfect test ratio only in 49 samples of core PC5101 and 16 samples of core PC5103, in which we could count more than 50 specimens; in all other samples this species is too rare.

2.2.4. Multivariate analyses of benthic foraminifera

The values of the Shannon-Wiener function (H') and the Buzas-Gibson evenness of (1969) were calculated for all analyzed samples, and combined with published data (Takata et al., 2011). We constructed rank-abundance curves (RAC) based on the relative abundance of each taxon for each sample (Webb et al., 2009; Webb and Leighton, 2011). We calculated RAC kurtosis using the Statistical programming environment R (R Development Core Team, 2010). In order to statistically evaluate faunal changes, we applied non-metric multi-dimensional scaling (MDS) on Bray-Curtis distances to the faunal data. A square-root transformed data matrix of relative abundance consisting of 18 taxa (those with at least 5% relative abundance in at least one sample) and 188 samples were analyzed by the statistical programming environment R, using the function from the Vegan Community ecology package (Oksanen et al., 2010). In order to consider the relationship between the MDS axis and each taxon, the correlation between stratigraphic changes in the score of each MDS axis and relative abundance of each taxon was examined.

3. Results

3.1. Age models

The oxygen isotope stratigraphy of cores PC5101 and PC5103 provided 17 and 12 age-tie points, respectively (Table 1; Supplements 1 and 2). Based on matching to the LR04 stack, our study intervals of these cores recorded the interval down to MIS 13 (Supplements 1 and 2). The benthic foraminiferal oxygen isotope

Table 1Tie points between depth and age of cores PC5101 and PC5103.

PC 5101				
Depth (cm)	Age (ka)			
6.21	3.11			
33.41	25.81			
87.00	64.69			
116.00	106.59			
136.23	125.33			
152.82	144.62			
187.91	195.62			
220.55	257.20			
255.09	307.58			
282.56	333.08			
309.76	364.49			
329.35	391.55			
351.65	415.81			
383.75	443.49			
417.75	470.85			
443.32	505.69			
543.41	620.45			

PC510	3
Depth (cm)	Age (ka)
7.22	7.21
70.76	68.50
102.53	122.06
156.24	188.49
164.50	218.45
241.06	342.48
257.76	379.56
281.01	416.64
329.81	474.83
364.85	539.72
395.97	582.47
414.63	614.40

data (*C. wuellerstorfi*) generally agree with the CaCO₃ stratigraphy. In contrast, the oxygen isotope data of the planktic foraminifera (*G. sacculifer*) in core PC5103 contain peaks (e.g., 30, 128–124, and 276 cm), which are inconsistent with the CaCO₃ stratigraphy (Supplements 2). We consider that the CaCO₃ variability indicates glacial—interglacial periods correctly (Farrell and Prell, 1989), whereas the low planktic oxygen isotope values probably represent local surface—water conditions. Our age model thus was based on the match with CaCO₃ data in core RC11-210 (Chuey et al., 1987). Sedimentation rates ranged from 0.53 to 1.38 cm kyr⁻¹ for core PC5101 and from 0.28 to 1.04 cm kyr⁻¹ for core PC5103.

3.2. Benthic foraminifera

Benthic foraminifera were present in all 59 samples in the lower part of core PC5101, 35 samples in the lower part of core PC5103, and in the 53 samples in the upper part of core PC5101 (Takata et al., 2011) and 41 samples in the upper part of core PC5103 (Takata et al., 2016). The abundance of benthic foraminifera (the number per gram) and BFAR fluctuated generally at glacial-interglacial periodicities (Fig. 2). In the lower parts of cores PC5101 and PC5103, Nuttallides umbonifer, Pullenia bulloides, Pullenia quinqueloba, Epistominella exigua, and Eilohedra levicula are common constituents, with Oridorsalis umbonatus, Cibicidoides wuellerstorfi, Melonis pompilioides and Melonis barleeanum (Figs. 2 and 3; Supplements 3). The faunal composition closely resembles those in the upper parts of cores PC5101 (Takata et al., 2011) and PC5103 (Takata et al., 2016), except for the abundance of Chilostomella ovoidea in one sample in core PC5101, where it is dominant (more than 30%; ~300 ka) (Fig. 2). The assemblages indicate (e.g., by the low relative abundance of infaunal indicator species of high productivity) that the food flux at the seafloor was never very large, despite the high primary productivity, as expected at the great depth (>4 km) of both sites (e.g., Altenbach et al., 1999).

Two MDS axes were recognized (Figs. 2 and 4; Supplements 4). The most common species are grouped into the four quadrants in a plot of MDS 1 vs MDS 2 (Fig. 4): (a) *E. exigua* is the only species to score negatively on MDS axis 1 and positively on axis 2, (b) *Nuttallides* spp. score negatively on both axes, as do (to a lesser degree) *Gyroidinoides subangulatus* and *Fursenkoina bradyi*, (c) Several *Pullenia* species, *Melonis* species, *C. ovoidea*, *E. levicula* and *Oridorsalis plummerae* score positively on both axes, and (d) The common cosmopolitan species *G. subglobosa*, *O. umbonatus*, *C. wuellerstorfi*, *Tosaia* sp., *Gyroidinoides* sp. A. as well as *Fissurina* species score positively on MDS axis 1 and negatively on axis 2.

In core PC5101, the score on MDS axis 1 was more negative at 360–310 ka and 280–200 ka, and that of axis 2 was more positive at 310–280 ka and 120–30 ka (Fig. 5). In core PC5103, the scores of MDS axes 1 and 2 were similar to those of PC5101, but in core PC5101 the scores on MDS axis 2 (variability of the food supply) were higher from 310 to 280 ka, whereas in core PC5103 they were higher at 120–30 ka (Fig. 6).

In both cores, the values of Shannon-Wiener (H') index (diversity) declined at ~330 ka (Fig. 5), but they diverged at 330-250 ka, with higher values in core PC 5103. At 120-10 ka the diversity was higher in core PC5101 (Figs. 5 and 6). Based on these data, we recognized Events 1, 2 and 3 in values of Shannon-Wiener (H') index at ~330, ~250 and ~120 ka, respectively (Figs. 5 and 6). The Buzas-Gibson evenness (1969) diverged between the two cores at ~310 ka and during 120-10 ka (Figs. 5 and 6), similar to the Shannon-Wiener (H') index. RAC kurtosis values were different between the two cores from 330 to 260 ka, with higher values in core PC5101 (Figs. 5 and 6). The structure of the community implies that few taxa were dominant in core PC5101 at ~300 ka (with C. ovoidea dominant in 1 sample at ~300 ka; Fig. 2). A few species were dominant from MIS 9 to MIS 8 in core PC5101 (Figs. 4 and 8). The relative abundance of *N. umbonifer* in core PC5101 decreased considerably at ~300 ka (Fig. 2), but there was no marked difference in Pullenia spp. between the two cores (Fig. 8). MIS 8 in core PC5101 was characterized by abundant (approximately 20%) E. exigua (Fig. 8).

3.3. Perfect test ratio of Globorotalia menardii

The perfect test ratio was similar in the two cores (Fig. 5), with more fluctuations after ~170 ka, and with more stable values prior to ~170 ka. The variation pattern of the perfect test ratio was roughly similar to that of other dissolution indices (foraminiferal fragmentation rate and foraminiferal dissolution index) in core WEC8803B-GC51 (1.3°N, 133.6°W, 4410 m water depth; LaMontagne et al., 1996), located close to core PC5101. Values also resemble the dissolution indices in core TT013-PC72 (0.1 °N, 140°W, 4298 m water depth; Fig. 11 of Thomas et al., 2000). Values in the latter are similar to our data but show larger fluctuations (most significantly after ~270 ka), and more glacial-interglacial variability overall.

4. Discussion

4.1. Faunal composition and structure of benthic foraminifera along ~131 W in the CEP

4.1.1. Faunal composition

We interpreted the scores of the characteristic species on the two MDS axes, using information in Loubere (1991, 1994, 1998),

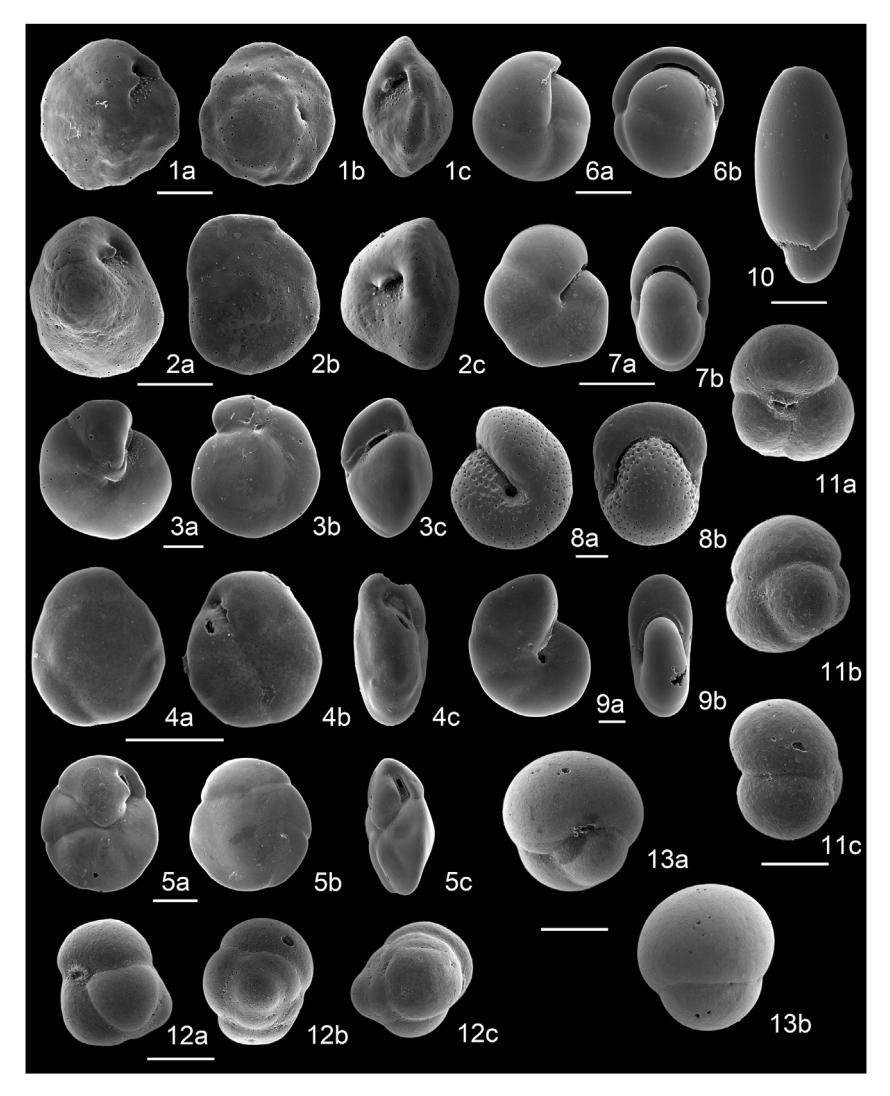


Fig. 3. Scanning electron micrographs of benthic foraminifera in cores PC5101 and PC5103. Scale bar = 100 μm. 1. Nuttallides umbonifer (Cushman) (core PC5101; 216–217 cm); 2. Nuttallides sp. A (core PC5101; 216–217 cm); 3. Oridorsalis umbonatus (Reuss) (core PC5101; 216–217 cm); 4. Eilohedra levicula (Resig) (core PC5101; 216–217 cm); 5. Epistominella exigua (Brady) (core PC5101; 216–217 cm); 6. Pullenia bulloides (d'Orbigny) (core PC5101; 216–217 cm); 7. Pullenia jarvisi Cushman (core PC5101; 216–217 cm); 8. Melonis pompilioides (Fichtel and Moll) (core PC5101; 212–213 cm); 9. Melonis barleeanum (Williamson) (core PC5101; 212–213 cm); 10. Chilostomella ovoidea Reuss (core PC5101; 252–253 cm); 11, 12. Tosaia hanzawai Takayanagi (core PC5101; 360–361 cm); 13. Sphaeroidina bulloides d'Orbigny (core PC5101; 216–217 cm).

Thomas et al. (1995), Altenbach et al. (1999), Gupta and Thomas (2003), Gooday (2003), Sun et al. (2006), and Jorissen et al. (2007). Based on the correlation between the score on MDS axis 1 and the relative abundance of each taxon (Supplements 4), Nuttallides umbonifer and Nuttallides sp. A are negatively correlated to MDS axis 1, whereas Oridorsalis umbonatus, Pullenia bulloides and Pullenia quinqueloba are positively related. Nuttallides umbonifer is fairly abundant in very deep waters between the lysocline and the CCD (Bremer and Lohmann, 1982; Mackensen et al., 1990, 1993; 1995; Schmiedl et al., 1997). In general, such deep waters contain only a very small fraction of the organic matter produced in the surface waters (Martin et al., 1987; Henson et al., 2012). This species thus thrives at an extremely low food supply (Loubere, 1991; Schmiedl et al., 1997). Nuttallides rugosa (probably equivalent to N. umbonifer) occurs at bathyal depths in the western Arabian Sea, where phytodetritus is deposited (Kurbjeweit et al., 2000). This species, however, might reproduce at times of little seasonal deposition, and it is commonly associated with a low, seasonal pulse in food supply (Gooday, 2003; Sun et al., 2006). Oridorsalis umbonatus and Pullenia spp. occur over a range of water depths and trophic conditions (e.g., Van Morkhoven et al., 1986), but generally at somewhat higher levels of food supply than *Nuttallides* spp. (e.g., Loubere, 1991; Altenbach et al., 1999). Thus, negative scores on MDS axis 1 indicate extremely low food supply, whereas positive scores indicate somewhat higher food supply.

Epistominella exigua has a negative score on MDS axis 1, and a positive score on MDS axis 2 (Fig. 4, Supplements 3). This species is abundant at locations with a highly seasonal input of phytodetritus from the surface ocean (Gooday, 1994; Smart et al., 1994; Thomas et al., 1995; Thomas and Gooday, 1996; Sun et al., 2006; Thomas, 2007). This species occurs commonly from the equator to ~6°N along ~131°W, responding to seasonal contrast in the chlorophyll-a concentration of the surface waters under the seasonal ITCZ movement, (Takata et al., 2016). Variability in input of phytodetritus may have occurred on other short time scales, such as the passage of Tropical Instability Waves (TIWs) (Willett et al., 2006) and ENSO variability, which could cause short-term variability in the food supply on time scales different from seasonality. Thus, we conclude that MDS axis 2 may be related to the variability in the food supply (higher variability at more positive scores).

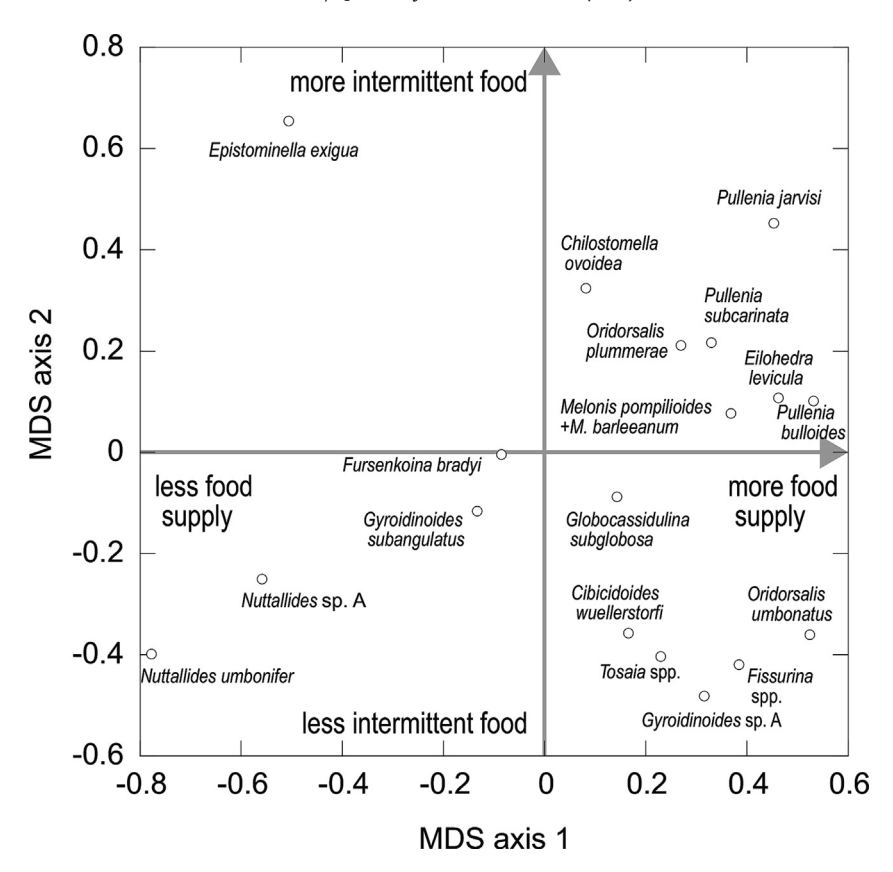


Fig. 4. Crossplot of correlation coefficients between MDS axes 1 and 2 and each taxon (including 53 data points from Takata et al. (2011) and 41 data points from Takata et al. (2016)). The data are listed in Supplements 4. Variation of benthic foraminiferal faunas were controlled primarily by MDS axis 1, specifically *Nuttallides umbonifer* (low food, low variability) and MDS axis 2, specifically *Epistominella exigua* (low food, high variability).

In summary, negative scores on MDS axis 1 indicate extremely low food flux, and positive scores a somewhat higher flux. Negative scores on MDS axis 2 indicate a fairly low variability (on time scales ranging from TIW passage to seasonal to ENSO), whereas positive scores indicate higher variability (Fig. 4).

4.1.2. Structure of the community

The Shannon-Wiener (H') index is significantly positively correlated with the evenness, negatively with RAC kurtosis in cores PC5101 and PC5103, based on Spearman's rank coefficient (Table 2). The correlation between MDS axis 1 and the Shannon-Wiener (H') index or evenness is significant in core PC5101 (Table 2). A more negative score on MDS axis 1 is related to higher abundance of *Nuttallides* spp., whereas a more positive score is characterized by higher abundances of species such as *P. bulloides*, *P. quinqueloba* and *O. umbonatus*. High scores on MDS axis 2 (high abundance of *E. exigua*) are correlated with relatively low values of the Shannon-Wiener (H') index as also observed elsewhere (Ohkushi et al., 2000) (Figs. 5 and 6).

The relationship between values on MDS axis 2 and the Shannon-Wiener (H') index (or evenness) differs between cores PC5101 and PC5103 (Table 2), because of the spike in values on MDS axis 2 at ~300 ka in core PC5101, at which time *E. exigua* was becoming more abundant in core PC5101 than in core PC5103 (Fig. 6). Both evenness and RAC kurtosis indicate that only a few species dominated the assemblages during MIS 9 to MIS 8, thus the community structure was controlled mainly by the abundance of a few dominant species, including *N. umbonifer and E exigua*, probably related to the amount and variability of the food supply from the surface ocean.

4.2. Faunal changes at ~131 W in the CEP since ~520 ka

We compared scores on MDS axis 1 (food supply) to values of other proxy data, which include the CaCO₃ and biogenic opal content and their MAR, BFAR, and the perfect test ratio of *G. menardii* in core PC5101 (Figs. 7 and 8). A shift in the relation of benthic foraminiferal assemblages to environmental proxies occurred at 118 cm (mid-MIS 5), based on the Horn's index of overlap between neighboring samples in core PC5101 (Takata et al., 2011). Therefore, we separately evaluated the correlation between scores on MDS axis 1 and other proxy data in different time intervals.

We defined the time intervals using the Shannon-Wiener (H') index in core PC5101 (Events 1 and 2; Fig. 6): Interval (c) 456.5–280.5 cm (520.8–331.2 ka: mainly MIS 13 to MIS 10; before Event 1); Interval (b) 276.5-220.5 cm (327.5-257.1 ka: mainly MIS 9 to MIS 8; between Events 1 and 2) at 288 cm and Interval (a) 216.5-0.5 cm (249.6-0 ka: mainly MIS 7 to MIS 1; after Event 2) at 218 cm (Table 2; Figs. 7 and 8). Interval (a) can be subdivided into Subintervals (a1 and a2) by Event 3 (at around the MIS 6/5 boundary, ~120 ka) (Fig. 5) (Takata et al., 2016). We do not further discuss this faunal transition here (Takata et al., 2011, 2016). Correlations between scores on MDS axis 1 and other proxy data were examined using Spearman's rank coefficient in these three intervals (Table 3). In Interval (a), the score on MDS axis 1 (food supply) is correlated negatively to the opal-MAR (P < 0.01) (Table 3; Fig. 6), whereas in Interval (b), MDS axis 1 is correlated negatively with the $CaCO_3$ content (P < 0.01), and correlations with the opal content and opal-MAR are positive (P < 0.01 and P < 0.05, respectively) (Table 3; Fig. 7). In Interval (c), MDS axis 1 was positively correlated

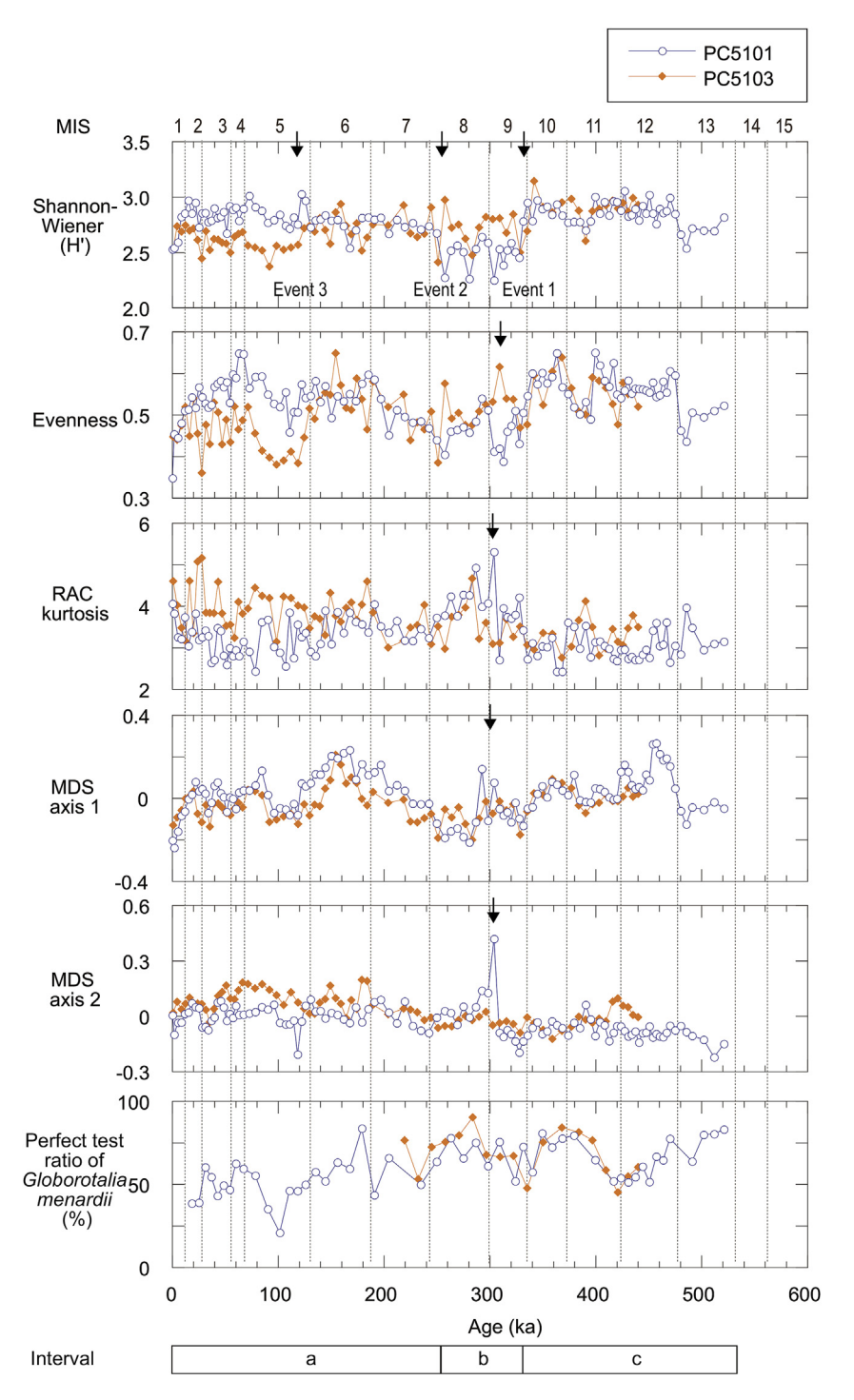


Fig. 5. Stratigraphic changes of Shannon-Wiener (H'), Buzas and Gibson evenness (1969), RAC kurtosis, multi-dimensional scaling (MDS) axes 1 and 2 (including 53 data points from Takata et al. (2011) and 41 data points from Takata et al., [2016]), and the perfect test ratio (%) of Globorotalia menardii of cores PC5101 and PC5103. Arrow shows the horizon of marked changes in value of each panel. The study period is subdivided in three intervals based on Shannon-Wiener (H') between the two cores (Events [a] and [b]; refer to section 4.2). Note that evenness, RAC kurtosis, and MDS axes 1 and 2 show differences between the two cores across ~300 ka.

with the $CaCO_3$ -MAR (P < 0.01) and with the $CaCO_3$ content (P < 0.05) (Table 3; Fig. 7).

The perfect test ratio of *G. menardii* generally reflects carbonate preservation (e.g., Kimoto et al., 2003). The correlation between the score on MDS axis 1 and the perfect test ratio was not significant throughout core PC5101, implying that post-mortem changes in faunal composition through carbonate dissolution are not significant. The lack of marked variation in the perfect test ratio of

G. menardii (Fig. 5) is probably due to the fact that our cores (4425 m and 4095 m water depths) are located at shallower depths than those in Fig. 4 of Farrell and Prell (1989) (below ~4600 m). We conclude that the correlation between the scores on MDS axis 1 and the carbonate/opal-MAR in our cores probably is not caused by carbonate dissolution.

The food supply from the surface ocean strongly affects the faunal composition of benthic foraminifera in the deep-sea

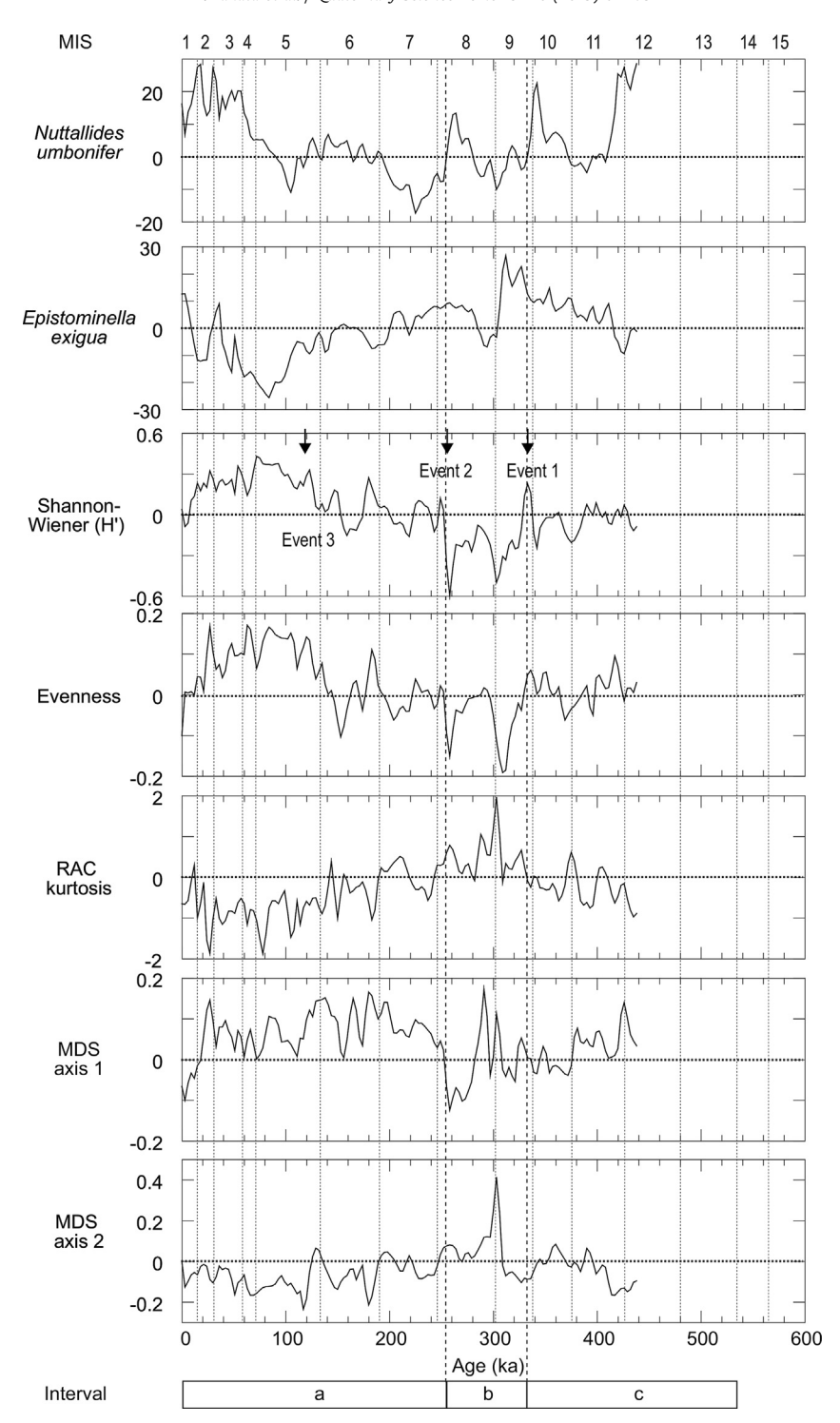


Fig. 6. Stratigraphic changes of the differences of relative abundance of *Nuttallides umbonifera* and *Epistominella exigua*, Shannon-Wiener (H'), Buzas and Gibson evenness (1969), RAC kurtosis, and multi-dimensional scaling (MDS) axes 1 and 2 in cores PC5101 and PC5103. The data in the cores were linearly interpolated data at 3 kyrs. The study period is subdivided into three intervals (a, b, and c) based on Shannon-Wiener (H') values in the two cores (Events [a] and [b]; section 4.2). Note that the evenness, RAC kurtosis, and MDS axes 1 and 2 show differences between the two cores across ~300 ka.

(Gooday, 2003; Jorissen et al., 2007). BFAR is a proxy for paleoproductivity, but only at constant export productivity (Herguera and Berger, 1991), and the correlation between scores on MDS axis 1 and BFAR is not statistically significant. Possibly, this lack of correlation is caused by the great water depth (>4000 m) at core PC5101, at which particulate organic matter (POM) from the surface ocean is largely consumed through remineralization within the

water column (e.g., Henson et al., 2012). Under such conditions, variations in BFAR may depend more on changes in the transfer efficiency of POM (export productivity) than on changes in primary productivity.

The negative correlation between scores on MDS axis 1 and opal-MAR was statistically significant in Interval (a). In that interval, the biotic response of benthic foraminifera suggests that less

Table 2Results of Spearman rank correlation of the indices at (a) core PC5101 and (b) core PC5103 (including 53 data from Takata et al. (2011) and 41 data from Takata et al. (2016)).

(a) core PC5101 Shannon-Wiener (H') Evenness	RAC kurtosis
MDS axis 1 $\rho = 0.49$ $\rho = 0.58$ $P < 0.01$ $P < 0.01$	$\rho = -0.17$ NS
MDS axis 2 $ \begin{array}{c} \rho = -0.04 \\ \text{NS} \end{array} \qquad \begin{array}{c} \rho = -0.03 \\ \text{NS} \end{array} $	ho = 0.20 $P < 0.01$
Evenness $\begin{split} \rho = 0.69 \\ \mathbf{P} < 0.01 \end{split}$	$ \rho = -0.48 P < 0.01 $
RAC kurtosis $ \rho = -0.55 \\ \textbf{P} < \textbf{0.01} $	
(b) core PC5103 Shannon-Wiener (H') Evenness	RAC kurtosis
MDS axis 1 $\rho = 0.54$ $\rho = 0.68$ $P < 0.01$ $P < 0.01$	$\begin{array}{c} \rho = -0.20 \\ NS \end{array}$
MDS axis 2 $\rho = -0.41$ $\rho = -0.32$ $P = 0.71$ $P < 0.01$	$ \rho = 0.47 \\ P < 0.01 $
$\Gamma = 0.71$ $\Gamma < 0.01$	
Evenness $\rho = 0.74$ $P < 0.01$	$ \rho = -0.55 $ $ \mathbf{P} < 0.01 $
Evenness $\rho = 0.74$,

food reached the seafloor at high opal-MAR, which appears to be counterintuitive. However, Henson et al. (2012) (in agreement with Klaas and Archer, 2002) suggested that biogenic opal grains (which are less dense than CaCO₃ skeletons) may have a negative effect on transfer efficiency of POM when summed over the full water depth: biogenic opal increases transfer efficiency of POM from the mixed layer to the thermocline, but the transfer efficiency decreases from the thermocline to the deep sea floor. Silica is undersaturated in the water column, thus opal skeletons are highly susceptible to dissolution, and their dissolution may negatively affect the sinking of POM lower in the water column. In contrast, scores on MDS axis 1 are positively related to CaCO₃ content and CaCO₃-MAR in Interval (c), which suggests that increased carbonate sedimentation affected food supply to the seafloor, in agreement with the argument that biogenic carbonate grains may ballast POM, thus increase transfer efficiency (Francois et al., 2002). These changes over time agree with Henson et al. (2012)'s argument that changes in photosynthetic communities strongly affect the amount of remineralization and thus the efficiency of transfer of POM through the water column.

Remineralization of POM is also affected by seawater temperature, with doubling of the activity of remineralizing bacteria with about 10 °C increase (e.g., John et al., 2013). However, a modeling study showed differences in temperature of <0.5 °C below ~1 km water depth around the equator from the LGM to today (Chikamoto et al., 2012), and bottom water temperatures have not changed greatly over our study interval (Siddall et al., 2010). We thus conclude that changes in remineralization over the studied interval in the CEP due to changes in temperature were not significant, and the shift in biotic response of benthic foraminifera over time may have been caused by changes in the ballasting effect of sinking POM, through changes in the MAR (paleo-flux) of carbonate and opal skeletons in the CEP in the mid-Brunhes dissolution interval (MBDI) (Fig. 9).

The cause of the change in correlation between MDS axis 1 and CaCO₃/opal-MARs Intervals (c) to (a) is not well understood. Coarse fraction (>63 μm)-MAR was more variable in Interval (a) than in Interval (c) (Fig. 7). In contrast, the fine fraction (<63 μm)-MAR does not show marked differences between Intervals (a) and (c). Given that coarse and fine fraction-MARs generally correspond to fluxes of planktic foraminifera and calcareous nannofossils, we suggest that the flux variations of planktic foraminifera and

calcareous nannofossils were similar in Interval (c), whereas the flux of planktonic foraminifera was more variable in Interval (a) than that of calcareous nannofossils. The more variable flux of planktic foraminifera in Interval (a) could have affected the relation between ballasting of POM by calcareous skeletons and benthic foraminiferal food supply, resulting in a more negative effect of ballasting of POM by siliceous plankton.

In Interval (b), scores on MDS axis 1 are negatively correlated to the CaCO₃ content, but positively to the opal content and its MAR. Therefore, we conclude that in Interval (b) there was no significant relation between scores on MDS axis 1 and carbonate/opal sedimentation. This interval is characterized by high scores on MDS axis 2 (Fig. 4), suggesting that benthic foraminiferal assemblages were mainly influenced by high variability in the food supply, rather than by the total amount of food and carbonate/opal sedimentation.

An important factor determining the food supply to the seafloor and benthic foraminiferal assemblages over time thus may have changed, with the change from carbonate sedimentation in Interval (c) to opal sedimentation in Interval (a), with Interval (b) transitional. This transition was gradual (~330 ka to ~250 ka), corresponding to the MBDI (Farrell and Prell, 1989). During this period benthic foraminiferal assemblages shifted from a linkage to carbonate sedimentation (Interval [c]) to a relation to opal sedimentation (Interval [a]). We regard this interval as a "regime shift", during which changes in surface paleoceanography affected food transfer to the deep-sea, as well as remineralization in the water column. We argue that a change in transfer efficiency of POM in the tropical Pacific Ocean, thus the efficiency of the biological pump, probably was an important feature of the MBDI.

4.3. Benthic for aminiferal fauna between ~2 N and ~6 N along ~131 W during MIS 9 and 7

In order to characterize the transition period (330–250 ka; Interval [b]) along ~131°W, we evaluated the differences between cores PC5101 and PC5103 in more detail (Figs. 6 and 8). The decrease in Shannon-Wiener (H') index from ~330 to 300 ka implies that benthic foraminiferal faunas were adversely affected at core PC5101, and the low values of BFAR in this core at ~300 ka suggest that the food supply decreased (Fig. 7). In core PC5101, E. exigua became abundant in MIS 8, just after the occurrence of extraordinary abundant C. ovoidea at ~300 ka (Fig. 8). Chilostomella ovoidea is a deep-infaunal species (Ohga and Kitazato, 1997; Kitazato et al., 2000), using degraded, more refractory organic matter rather than fresh phytodetritus (Nomaki et al., 2006; Gooday et al., 2008). We suggest that E. exigua lived near the sediment surface digesting fresh phytodetritus, whereas C. ovoidea lived beneath the sediment surface. Therefore, a combination of a decrease in food supply and enhanced variability of the food supply might have strongly affected the benthic foraminiferal fauna prior to MIS 8.

High RAC kurtosis at ~300 ka also supports the hypothesis that conditions were more stressed for the benthic foraminiferal fauna in core PC5101. We thus conclude that phytodetritus species, as opportunists, transiently became abundant in core PC5101 whereas abundance of other species declined at ~300 ka. Hence, we subdivide transition Interval (b) in core PC5101 into an early and later part, with the boundary at ~300 ka (Fig. 8). The early part of transition Interval (b) (~330—300 ka) was characterized by the gradual deterioration of conditions for benthic foraminiferal fauna, probably due to less stable food supply (based on Shannon-Wiener (H') index and BFAR), whereas the later part (~300—250 ka) was characterized by enhanced variability of the food supply.

We thus explain the divergence in benthic foraminiferal fauna between cores PC5101 and PC5103 in transitional Interval (b) as

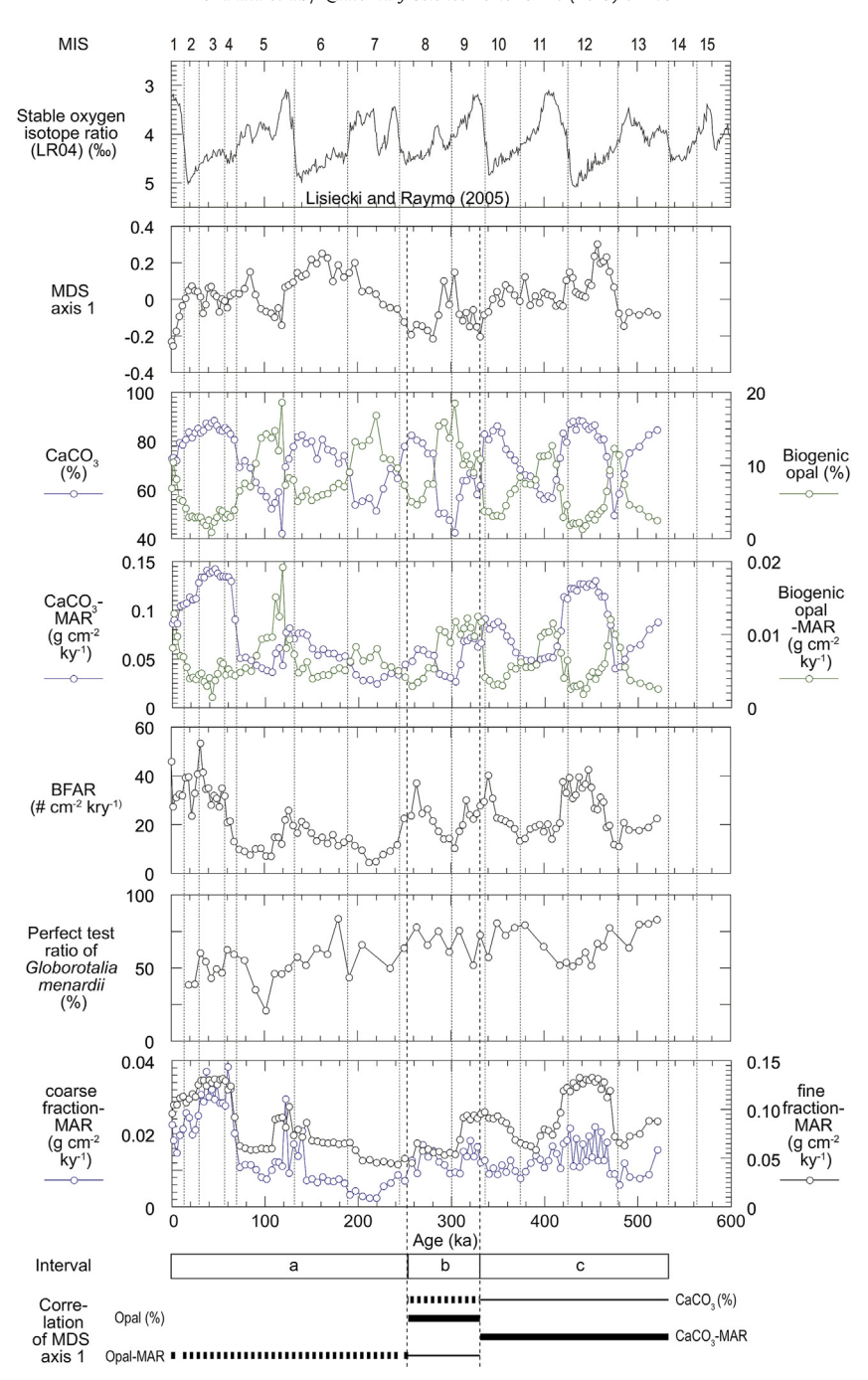


Fig. 7. Stratigraphic changes of oxygen isotope value of benthic foraminifera (Lisiecki and Raymo, 2005), multi-dimensional scaling (MDS) axis 1 (including 53 data from Takata et al. (2011)), CaCO₃ and biogenic opal contents (%) of bulk sediments (Khim et al., 2012), mass accumulation rate of CaCO₃ and biogenic opal, Benthic Foraminiferal Accumulation Rate (BFAR) (including 53 data points from Takata et al. (2011)), the perfect test ratio of Globorotalia menardii (%), and coarse and fine fraction-MARs of core PC5101. The results of Spearman's rank correlation in Table 3 were shown by the line drawing below the panels: solid and dashed line: positive and negative correlations, respectively, thick and narrow lines: P < 0.01 and P < 0.05, respectively. Intervals (a), (b) and (c) refer to section 4.2. The relationship between MDS axis 1 of benthic foraminifera and CaCO₃/biogenic opal-MARs shifted from positive correlation with CaCO₃-MAR in the Interval (c) to negative correlation with biogenic opal-MAR in the Interval (a). This suggests that biotic response of benthic foraminifera happened across ~300 ka due to change in ballasting of POM by biominerals.

follows: (1) the species diversity (Shannon-Wiener [H'] index) diverged from ~330 ka, (2) The benthic foraminiferal fauna in core PC5101 was negatively affected by a low food supply at ~300 ka, recovering afterward, and (3) the difference in species diversity between the two cores was reduced after ~250 ka. Such a faunal transition has not been recognized in other studies of benthic foraminifera in the Pacific Ocean (Ohkushi et al., 2000; Zhang et al., 2007), probably because this change was restricted to the

equatorial region. In addition, *E. exigua* was more abundant at ~6°N than at ~2°N after ~120 ka (Takata et al., 2016), but this was opposite in the late part of Interval (b), although variations in abundance of the most characteristic taxa were similar in both cores (Fig. 2).

The seasonal movement of the trade winds results in seasonal variation in primary productivity at the northern margin of the ITCZ during winter to spring (e.g., Kim et al., 2011), possibly influenced by the occurrence of TIWs (e.g. Legeckis et al., 2004). The increase in

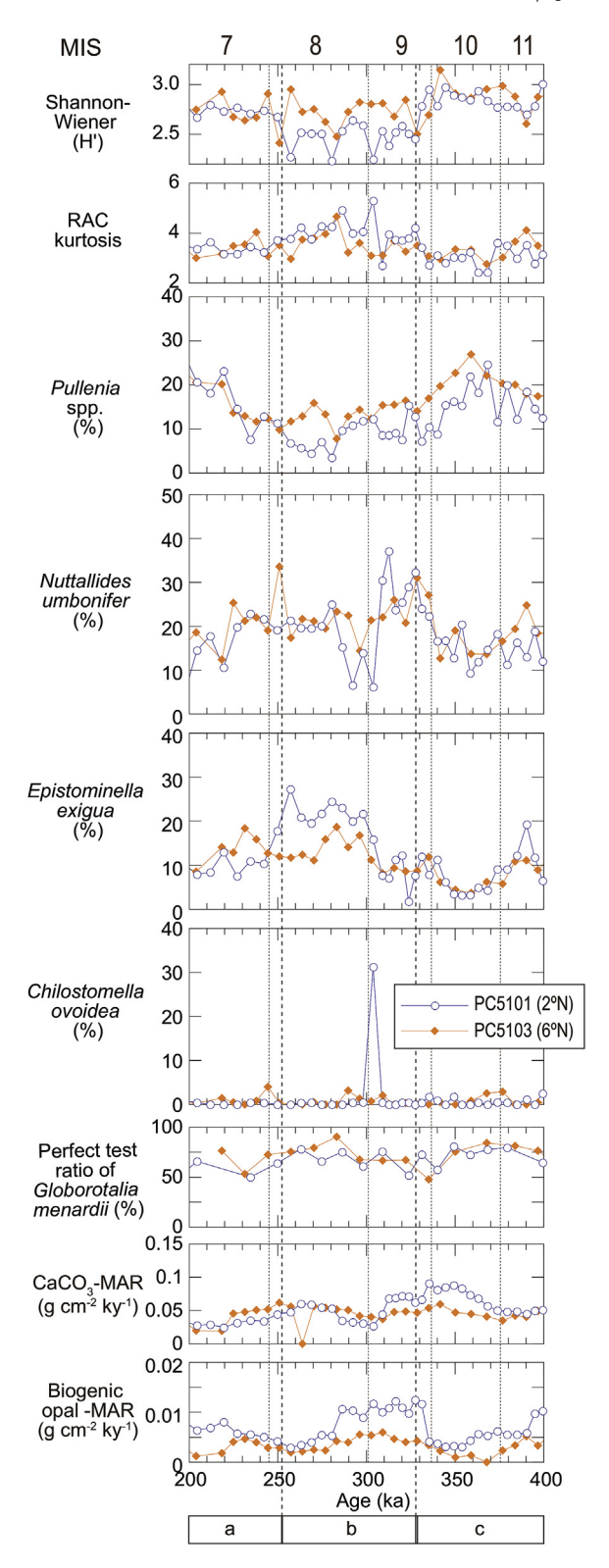


Fig. 8. Stratigraphic changes of Shannon-Wiener (H'), RAC kurtosis, relative abundances of five characteristic benthic foraminifera (including 53 data points from Takata et al. (2011) and 41 data points from Takata et al., [2016]), the perfect test ratio (%) of *Globorotalia menardii*, and mass accumulation rate of CaCO₃ and biogenic opal (Khim et al., 2012, 2015) of cores PC5101 and PC5103 during MIS 12 to MIS 7. Intervals (a), (b) and (c) refer to section 4.2. Interval (b) with lower Shannon-Wiener (H') in core PC5101 was subdivided into an early and later part at ~300 ka with the dominance of *Chilostomella ovoidea* in core PC5101. The early part of the Interval (b) (~330–300 ka) is characterized by the decrease of some taxa (e.g., *Nuttallides umbonifer*) in core PC5101, whereas the later part of the interval (b) (~300–250 ka) is characterized by the occurrence of common *Epistominella exigua* in core PC5101.

abundance of E. exigua further north (toward ~6°N) might be explained by seasonal variation in productivity with the migration of the ITCZ (Takata et al., 2016). Thus, the latitudinal difference in variability of the food supply in the later part of transition Interval (b) was opposite to that after ~120 ka. The opposite trend in relative abundance of E. exigua in the later part of Interval (b) relative to that at the present day could be explained by a southward displacement of the ITCZ (e.g., Rea, 1994) to ~2°N, so that the location (~6°N) of core PC5103 would be away from the equatorial sediment bulge (e.g., Lyle, 2003). However, there was no marked decline in the CaCO₃-MAR in core PC5103 (Fig. 7). Instead, an increased variability (especially its seasonality) in the ITCZ position without net latitudinal displacement might account for the reversed latitudinal pattern in abundance of E. exigua between MIS 8 and the interval after ~120 ka. In addition, variability on other than seasonal time scales, such as active motion of TIWs (e.g., Willett et al., 2006) or ENSO variability, could have contributed to variability in food supply. Thus, Interval (b), i.e. the transitional period in the biotic response of benthic foraminifera, could have been a period of temporal disturbance of the latitudinal variation of the ITCZ along ~131°W in the CEP, as suggested by Yu et al. (2017) for MIS 14 in the EEP. Such a temporal disturbance in the latitudinal variation of the ITCZ along ~131°W in the CEP could have been related to temporal reorganization of oceanic and atmospheric circulation in the Equatorial Pacific Ocean (e.g., changes of Walker Circulation/Hadley Circulation strength: Chiyonobu, 2009; southward ITCZ displacement: Yamazaki, 2012).

Longitudinal variations in the equatorial upwelling zone with changes in the carbonate-rich sediment bulge along the equator (e.g., Fig. 7 of Theyer et al., 1985, Fig. 14 of Lyle, 2003) might have been important, in addition to latitudinal variation. CaCO₃-MAR is generally higher in the eastern part of the carbonate-rich sediment bulge, where it is also broader (Lyle, 2003). A westward movement of the carbonate-rich sediment bulge might explain both the continuous CaCO₃ sedimentation and an episodic food supply in our study area. Unfortunately, there are no data available to evaluate detailed longitudinal variations in sediment geochemistry and benthic foraminiferal fauna. Khim et al. (2012) reported large-scale longitudinal variation of carbonate and biogenic opal contents in the equatorial Pacific (~131°W and ~164°E, respectively), and noted higher amplitude variations in biogenic opal content at core PC5101 than in core PC313 after ~350 ka, suggesting there was large-scale longitudinal variation in production of calcareous/siliceous plankton. Future studies focusing on longitudinal variations during the MBDI are needed to provide information on longitudinal versus latitudinal variability.

4.4. Shift in biotic response of benthic foraminifera through ballasting of POM

Deep-sea benthic foraminifera live in highly food-limited environments, and the food supply and its variability thus have a strong influence on their assemblage composition (e.g., Smart et al., 1994; Gooday, 2003; Jorissen et al., 2007). Benthic foraminiferal assemblages can react only to organic matter that reaches the seafloor, and the percentage of primary-produced organic matter reaching the seafloor is very small (0.01–1.0%; Murray et al., 1996). The decline in food flux with depth is not a simple logarithmic function of depth (as had been proposed; e.g., Martin et al., 1987), but highly variable and influenced by the structure of the phytoplankton community (Boyd and Trull, 2007; Henson et al., 2012; Arndt et al., 2013), as well as by the intensity of remineralization, which may depend on seawater temperature (John et al., 2013; Ma et al., 2014).

•		•		•		
Interval (age)	MDS axis1 vs. CaCO3 (%)	MDS axis 1 vs. opal (%)	MDS axis 1 vs. CaCO3-MAR	MDS axis 1 vs. opal-MAR	MDS axis 1 vs. BFAR	MDS axis 1 vs. perfect test ratio
(a) 216.5–0.5 cm	$\rho = 0.07$	$\rho = -0.13$	$\rho = -0.12$	$\rho = -0.37$	$\rho = -0.24$	$\rho = 0.25$
(249.6-0 ka)	NS	NS	NS	P < 0.01	NS	NS
(b) 276.5-220.5 cm	$\rho = -0.70$	$\rho = 0.73$	$\rho = -0.09$	$\rho = 0.64$	$\rho = -0.49$	$\rho = -0.43$
(327.5-257.1 ka)	P < 0.01	P < 0.05	NS	P < 0.05	NS	NS
(c) 456.5-280.5 cm	$\rho = 0.33$	$\rho = -0.27$	$\rho = 0.55$	$\rho = 0.02$	$\rho = 0.28$	$\rho = -0.28$
(520.8-331.2 ka)	P < 0.05	NS	P < 0.01	NS	NS	NS
Whole interval	$\rho = 0.22$	$\rho = -0.24$	$\rho = 0.15$	$\rho = -0.22$	$\rho = -0.12$	$\rho = -0.04$
(520.8-0 ka)	P < 0.05	P < 0.01	NS	P < 0.05	NS	NS

Table 3Results of Spearman rank correlation among MDS axis 1 and other proxies of core PC5101 among the three intervals

4.4.1. Impact of ballasting of POM to the efficiency of the biological pump in the ocean

The efficiency of transport of organic matter to greater depths depends on ballasting of POM by mineral matter, either by carbonate or siliceous biogenic material (Francois et al., 2002; Klaas and Archer, 2002; Katz et al., 2005) or windblown dust (Ittekkot, 1993). There is no agreement as to the relative significance of ballasting by these components (Passow, 2004).

Not much attention has been paid to potential faunal changes of Cenozoic benthic foraminiferal assemblages as a response to variability in ballasting minerals (e.g., Takata et al., 2018). We argue that ballasting of POM by biominerals could be one of the important factors for understanding faunal change in benthic foraminifera in the EEP, where the proportions of calcareous and siliceous plankton have fluctuated significantly over time (e.g., Khim et al., 2015).

In the MBDI, the calcareous nannoplankton species group Gephyrocapsa was dominant and may have contributed to ballasting POM in the deep ocean (Barker et al., 2006). Such intensification of the biological pump through ballasting of POM with coccoliths could have increased carbonate saturation of bottom water. A longterm trend (several hundreds of kyr-order) of changes in carbonate saturation is expressed in gradual shoaling followed by gradual deepening of the CCD ~325 ka in the EEP during the late Quaternary (Fig. 4 of Farrell and Prell, 1989), in addition to 100 kyr-order cyclicity. Our results suggest that dominant ballasting of POM switched from carbonate grains to biogenic opal grains during the MBDI. The positive relationship between MDS axis 1 and carbonate sedimentation in Interval (c) thus can be seen as supporting Barker et al. (2006). In contrast, the negative relation between MDS axis 1 and opal sedimentation in Interval (a) may be partly explained by increased carbonate saturation of bottom water in the late part of the MBDI through a decline of the efficiency in ballasting of POM (Fig. 4 of Farrell and Prell, 1989).

Many studies have pointed out the co-occurrence of paleoceanographic changes in the surface and deep oceans during the MBDI (Farrell and Prell, 1989; Barker et al., 2006). Farrell and Prell (1989) suggested that changes in atmospheric circulation, such as aeolian dust supply, could have been the cause of this coupling of surface and deep paleoceanographic events. We suggest that changes in ballasting of POM by biominerals may be an important factor affecting the function of the biological pump, and such changes in ballasting could have contributed to the correlation between surface and deep paleoceanographic changes in the MBDI.

4.4.2. Influence of surface paleoceanographic changes on the deep ocean in the equatorial Pacific Ocean through ballasting of POM

The start of Interval (a) was almost coeval with a decrease in relative abundance of very small coccoliths (<2.5 μ m) and an

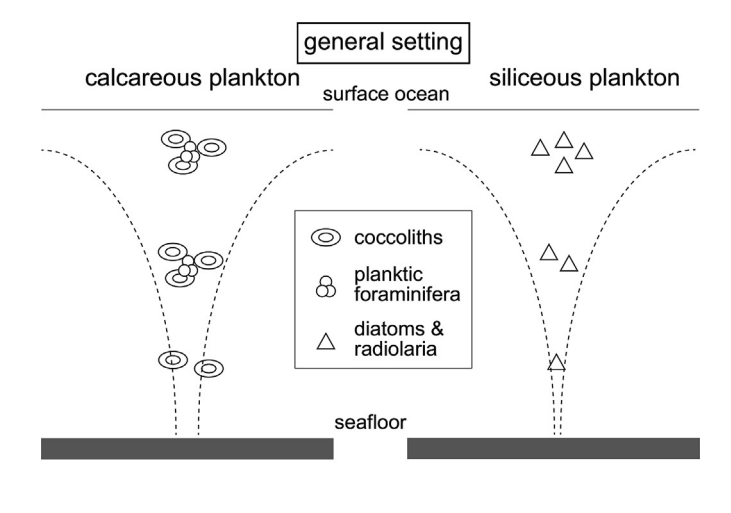
increase in relative abundance of warm-water coccoliths at ODP Site 846 (~3°S and ~95°W), across the MIS 8/7 boundary (~250 ka) (Chiyonobu et al., 2006; Chiyonobu, 2009). Our study area (~131°W) is far from ODP Site 846, but changes in primary producers may have affected large areas of the EEP at about ~250 ka. In contrast, the E—W gradient in SST in the Equatorial Pacific Ocean did not weaken distinctly from MIS 7, due to other long-term trends (i.e., the decrease toward ~200 ka and the subsequent increase; De Garidel-Thoron et al., 2005; Horikawa et al., 2010). Thus, weakening of the Walker Circulation might be a possible explanation for the decline in ballasting of POM by opal skeletons in Interval (a).

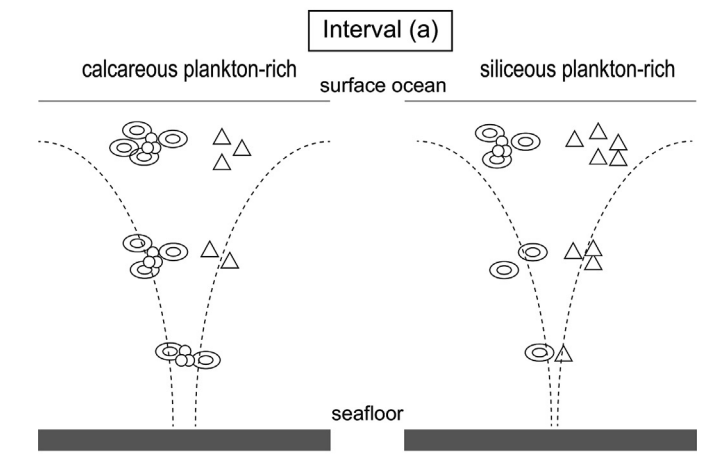
At ODP Site 846, the calcareous nannoplankton flora shows transitional features during MIS 8 related to an intensity of the equatorial upwelling (Chiyonobu, 2009). The change of benthic foraminifera in MIS 8 thus was probably related to a change in ITCZ, possibly with changes in its seasonal (or interannual) variation patterns (Section 4.3). Latitudinal variations in the seasonal pattern of the ITCZ might explain the changes in phytoplankton community, leading to a decline in ballasting of POM by opal skeletons as compared to carbonate skeletons. We must consider the regional paleoceanography in the tropical Pacific, in addition to global oceanographic changes (Barker et al., 2006), in order to understand paleoceanographic changes in the MBDI. We thus argue that an enhanced biological pump through ballasting of POM by biominerals (Barker et al., 2006) probably was combined with the weakening of the Walker Circulation and/or latitudinal changes in the ITCZ across the MBDI. Our results suggest that a change in the Walker Circulation and ITCZ may have caused changes in the deep oceans through changes in ballasting of POM by biominerals.

Other changes in surface paleoceanography might have affected the variability of the food supply; for example, the intensity of equatorial upwelling or the nutrient content of upwelled waters may have decreased at ~95°W after MIS 8 (Chiyonobu et al., 2006). If the latter phenomenon happened, primary productivity may have decreased without changes in atmospheric circulation and in position of the ITCZ. In addition, we may also need to consider longitudinal variation in regional surface oceanography, such as intensification of southern counter flow in the EEP (e.g., South Equatorial Counter Current). Further studies are needed to clarify the latitudinal (and longitudinal) variation in surface paleoceanography in the Equatorial Pacific Ocean.

5. Conclusions

Investigation of upper Quaternary benthic foraminifera in two sediment cores (PC5101 and PC5103) along ~131°W in the Central Equatorial Pacific Ocean led to the following conclusions:





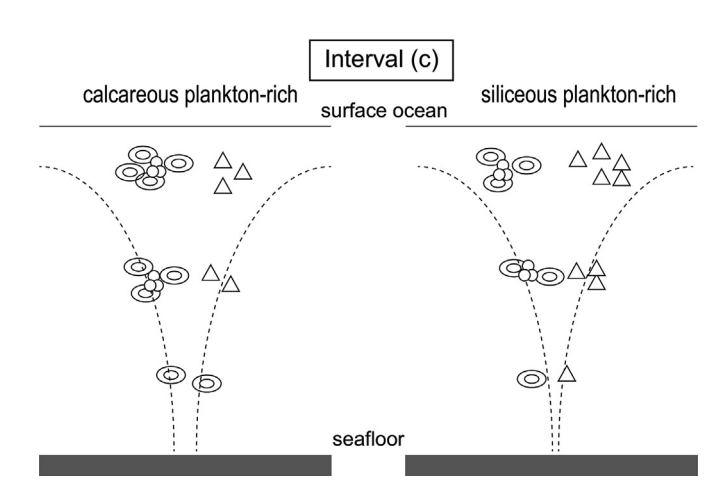


Fig. 9. Schematic diagrams depicting ballasting of particulate organic matter (POM) by calcareous/siliceous plankton. The dashed curves in each panel show the decreasing of POM down the water column. The upper panels show ballasting of POM in general, whereas the middle and lower panels show ballasting of POM during Intervals (a) and (c), respectively. The downward exponential-shape dashed lines show remineralization of POM with depth. The transfer efficiency of POM is affected by ballasting of biominerals: calcareous plankton (coccoliths and planktic foraminifera) and siliceous plankton (diatom and radiolaria). Carbonate grains probably are a more efficient ballasting material than opal grains. The calcareous plankton-rich and siliceous plankton-rich periods alternated over time.

- (1) We recognized two MDS axes in the benthic foraminiferal assemblages. Scores on MDS axis 1 are related to variability in overall food supply, from extremely low food (more negative scores) to slightly higher food (more positive scores). Scores on MDS axis 2 are related to the variability of the food supply (more positive score—increased variability). MDS axis 1 is correlated significantly to the Shannon-Wiener (H') diversity index, evenness and RAC kurtosis, suggesting that late Quaternary benthic foraminiferal faunas were controlled primarily by a few dominant species loading on MDS axis 1, specifically *Nuttallides umbonifer* (low food, low variability) and MDS axis 2, specifically *Epistominella exigua* (low food, high variability).
- (2) The scores on MDS axis 1 were compared with sediment geochemistry proxies in core PC5101, in which benthic foraminiferal assemblages switched from a positive relation to carbonate sedimentation (MIS 13 to MIS 10) to a negative relation to opal sedimentation (MIS 7 to MIS 1), with a transitional period (MIS 9 to MIS 8). Thus, carbonate was probably a more efficient ballasting material than opal, as seen in food supply to the benthic foraminifera in the Central Equatorial Pacific Ocean.
- (3) There are latitudinal differences in benthic foraminiferal abundances, species diversity (Shannon-Wiener [H'] index), and evenness between the two cores during the transitional period (MIS 9–8). *Epistominella exigua*, indicating a highly variable food supply, is more abundant at the northern margin of seasonal ITCZ movement than at the equator at the present day, whereas this was reversed during MIS 8. Such a reversal of latitudinal distribution may be attributed to an enhanced variability in food supply near the equator, related to the increased seasonal (or interannual) motion of trade winds, without net displacement of the mean ITCZ position.

Acknowledgements

We thank Prof. R. Nomura (Shimane University) for his advice in identification of benthic foraminifera. We appreciate K. Kimoto (JAMSTEC) for his comment about the perfect test ratio of *Globorotalia menardii*. We are indebted to the editor and two anonymous reviewers for their useful comments to improve the manuscript. This research was supported by the research programs of the Korea Institute of Ocean Science and Technology (PE99583 to BKK), National Research Foundation (2016R1A2B4008256, 2019R1A2C1007701 to BKK), and partly by the National Science Foundation (OCE 1736538 to ET).

Appendix A. Supplementary data

Supplementary data to this article can be found online at https://doi.org/10.1016/j.quascirev.2019.02.030.

References

Acker, J.G., Leptoukh, G., 2007. Online analysis enhances use of NASA Earth science data". Eos, Trans. AGU. 88 (2), 14–17, 9 January 2007.

Altenbach, A.V., Pflaumann, U., Schiebel, R., Thies, A., Timm, S., Trauth, M., 1999. Scaling percentages and distributional patterns of benthic Foraminifera with flux rates of organic carbon. J. Foraminifer. Res. 29, 173–185.

Amador, J.A., Alfaro, E.J., Lizano, O.G., Magaña, V.O., 2006. Atmospheric forcing of the eastern tropical Pacific: a review. Prog. Oceanogr. 69, 101–142.

Arndt, S., Jorgensen, B.B., LaRowe, D.E., Middleburg, J.J., Pancost, R.D., Regnier, P., 2013. Quantifying the degradation of organic matter in marine sediments: a review and synthesis. Earth Sci. Rev. 123, 53–86.

Barker, S., Archer, D., Booth, L., Elderfield, H., Hendericks, J., Rickaby, R.E.M., 2006. Globally increased pelagic carbonate production during the Mid-Brunhes dissolution interval and the CO₂ paradox of MIS11. Quat. Sci. Rev. 25, 3278–3293.

- Boyd, P.W., Trull, T.W., 2007. Understanding the export of biogenic particles in ocean waters: is there consensus? Prog. Oceanogr. 72, 276–312.
- Bremer, M.L., Lohmann, G.P., 1982. Evidence for primary control of the distribution of certain Atlantic Ocean benthonic foraminifera by degree of carbonate saturation. Deep-Sea Res. 29, 987-998.
- Buzas, M.A., Gibson, T.G., 1969. Species diversity: benthonic foraminifera in western North Atlantic. Science 163, 72–75.
- Chavez, F.P., Barber, R.T., 1987. An estimate of new production in the equatorial Pacific. Deep-Sea Res. Part A 34, 1229-1243.
- Chikamoto, M.O., Menviel, L., Abe-Ouchi, A., Ohgaito, R., Timmermann, A., Okazaki, Y., Harada, N., Oka, A., Mouchet, A., 2012. Variability in North Pacific intermediate and deep water ventilation during Henrich events in two coupled climate models, Deep-Sea Res, Part II 61-64, 114-126.
- Chiyonobu, S., 2009. Upwelling strength and water mass structure changes in the equatorial Pacific Ocean during the last 550 kyr as recorded by calcareous nannofossil assemblages, Fossils 86, 34–44 (in Japanese with English abstract).
- Chiyonobu, S., Sato, T., Narikiyo, R., Yamasaki, M., 2006. Floral changes in calcareous nannofossils and their paleoceanographic significance in the equatorial Pacific Ocean during the last 500000 years. Isl. Arc 15, 476–482.
 Chuey, J.M., Rea, D.K., Pisias, N.G., 1987. Late Pleistocene paleoclimatology of the
- central equatorial Pacific: a quantitative record of eolian and carbonate deposition. Quat. Res. 28, 323–339.
- Clark, P.U., Archer, D., Pollard, D., Blum, J.D., Rial, J.A., Brovkin, V., Mix, A.C., Pisias, N.G., Roy, M., 2006. The middle Pleistocene transition: characteristics, mechanisms, and implications for long-term changes in atmospheric pCO₂. Quat. Sci. Rev. 25, 3150-3184.
- De Garidel-Thoron, Rosenthal, T.Y., Bassinot, F., Beaufort, L., 2005. Stable sea surface temperatures in the western Pacific warm pool over the past 1.75 million years. Nature 433, 294-298.
- Farrell, J.W., Prell, W.L., 1989. Climatic change and CaCO₃ preservation: an 800000 year bathymetric reconstruction from the central Equatorial Pacific Ocean. Paleoceanography 4, 447-446.
- Farrell, J.W., Prell, W.L., 1991. Pacific CaCO $_3$ preservation and $\delta^{18}O$ since 4 Ma: paleoceanographic and paleoclimatic implications. Paleoceanography 6, 485-498
- Francois, R., Honjo, S., Krishfield, R., Manganini, S., 2002. Factors controlling the flux of organic carbon to the bathypelagic zone of the ocean. Glob. Biogeochem. Cycles 16. https://doi.org/10.1029/2001GB001722.
- Gooday, A.J., 1994. The biology of deep-sea foraminifera: a review of some advances and their applications in paleoceanography. Palaios 9, 14-31.
- Gooday, A.J., 2003. Benthic foraminifera (Protista) as tools in deep-water paleoceanography: a review of environmental influences on faunal characteristics. Adv. Mar. Biol. 46, 1-90.
- Gooday, A., Nomaki, H., Kitazato, H., 2008. Modern deep-sea benthic foraminifera: a brief review of their morphology-based biodiversity and trophic diversity. In: Autin, W.E.N., James, R.H. (Eds.), Biogeochemical Controls on Paleoceanographic Environmental Proxies. Geol. Soc, vol. 303. Spec. Pub., London, pp. 97-119.
- Gupta, A., Thomas, E., 2003. Initiation of northern hemisphere glaciation and strengthening of the northeast Indian monsoon: ocean Drilling program site 758, eastern equatorial Indian ocean. Geology 31, 47-50.
- Henson, S.A., Sanders, R., Madsen, E., 2012. Global patterns in efficiency of particulate organic carbon export and transfer to the deep ocean. Glob. Biogeochem. Cycles 26, GB1028. https://doi.org/10.1029/2011GB004099.
- Herguera, J.C., Berger, W., 1991. Paleoproductivity from benthonic foraminifera abundance glacial to postglacial change in the west-equatorial Pacific. Geology 19, 1173-1176.
- Honjo, S., Dymond, J., Collier, R., Manganini, S.J., 1995. Export production of particles to the interior of the equatorial Pacific Ocean during the 1992 EqPac experiment. Deep-Sea Res. Part II 42, 831-870.
- Horikawa, K., Murayama, M., Minagawa, M., Kato, Y., Sagawa, T., 2010. Latitudinal and downcore (0-750 ka) changes in n-alkane chain lengths in the eastern equatorial Pacific. Quat. Res. 73, 573-582.
- Ittekkot, V., 1993. The abiotically driven biological pump in the ocean and shortterm fl uctuations in atmospheric CO2 contents: global and Planet. Change 8, 17-25. https://doi.org/10.1016/0921-8181(93)90060-2.
- Jin, F.F., 1996. Tropical ocean-atmosphere interaction, the pacific cold tongue, and the El niño-southern oscillation. Science 274, 76-78.
- John, E.H., Pearson, P.N., Coxall, H.K., Birch, H., Wade, B.S., Foster, G.L., 2013. Warm ocean processes and carbon cycling in the Eocene. Philos. Trans. Royal Soc. A 371, 20130099. https://doi.org/10.1098/rsta.2013.0099.
- Jones, R.W., 1994. The Challenger Foraminifera. Oxford University Press, Oxford.
- Jorissen, J.J., Fontanier, C., Thomas, E., 2007. Paleoceanographical proxies based on deep-sea benthic foraminiferal assemblage characteristics. In: Hillaire-Marcel, C., de Vernal, A. (Eds.), Proxies in Late Cenozoic Paleoceanography, vol. 1. Elsevier, pp. 263-326.
- Katz, M.E., Wright, J.D., Miller, K.G., Cramer, B.S., Fennel, K., Falkowski, P., 2005. Biological overprint of the geological carbon cycle. Mar. Geol. 217, 323-338. https://doi.org/10.1016/j.margeo.2004.08.005.
- Khim, B.K., Kim, H.J., Cho, Y.S., Chi, S.B., Yoo, C.M., 2012. Orbital variations of biogenic CaCO₃ and opal abundance in the western and central Equatorial Pacific Ocean during the late Quaternary. Terr. Atmos. Ocean Sci. 23, 107-117.
- Khim, B.K., Yoo, C.M., Kim, H.J., Hyeong, K., Takata, H., Kim, S., Chi, S.B., Ko, Y.T., 2015. Biogenic CaCO₃ and opal depositions and their latitudinal comparison during the past 600 ka in the central equatorial Pacific. Terr. Atmos. Ocean Sci. 26, 441-450.

- Kim, H.J., Kim, D., Yoo, C.-M., Chi, S.-B., Khim, B.-K., Shin, H.-R., Hyeong, K., 2011. Influence of ENSO variability on sinking-particle fluxes in the northeastern equatorial Pacific. Deep-Sea Res. Part I 58, 865-874.
- Kimoto, K., Takaoka, H., Oda, M., Ikehara, M., Matsuoka, H., Okada, M., Oba, T., Taira, A., 2003. Carbonate dissolution and planktonic foraminiferal assemblages observed in three piston cores collected above the lysocline in the western equatorial Pacific. Mar. Micropaleontol. 47, 227–251.
- Kitazato, H., Shirayama, Y., Nakatsuka, T., Fujiwara, S., Shimanaga, M., Kato, Y., Okada, Y., Kanda, J., Yamaoka, A., Masuzawa, T., Suzuki, K., 2000. Seasonal phytodetritus deposition and response of bathyal benthic foraminiferal populations in Sagami Bay, Japan: preliminary results from "Project Sagami 1996-1999. Mar. Micropaleontol. 40, 135–149.
- Klaas, C., Archer, D.E., 2002. Association of sinking organic matter with various types of mineral ballast in the deep sea; implications for the rain ratio. Glob. Biogeochem. Cycles 16, 1116. https://doi.org/10.1029/2001GB001765.
- Kurbieweit, F., Schmiedl, G., Schiebel, R., Hemleben, Ch. Pfannkuche, O., Wallmann, K., Schäfer, P., 2000. Distribution biomass and diversity of benthic foraminifera in relation to sediment geochemistry in the Arabian Sea, Deep-Sea Res. Part II 47, 2913-2955.
- LaMontagne, R.W., Murray, R.W., Wei, K.-W., Leinen, M., Wang, C.-H., 1996. Decoupling of carbonate preservation, carbonate concentration, and biogenic accumulation: a 400 kyr-record from the central equatorial Pacific Ocean. Paleoceanography 11, 553-562.
- Legeckis, R., Brown, C.W., Bonjean, F., Johnson, E.S., 2004. The influence of tropical instability waves on phytoplankton blooms in the wake of the Marquesas Islands during 1998 and on the currents observed during the drift of the Kon-Tiki in 1947. Geophys. Res. Lett. 31, L23307. https://doi.org/10.1029/ 2004GL021637
- Lisiecki, L.E., Lisiecki, P.A., 2002. Application of dynamic programming to the correlation of paleoclimate records. Paleoceanography 17 (D4), 1049. https:// doi.org/10.1029/2001PA000733, 2002.
- Lisiecki, L.E., Raymo, M.E., 2005. A Pliocene-Pleistocene stack of 57 globally distributed benthic δ^{18} O records. Paleoceanography 20, PA1003. https://doi.org/ 10.1029/2004PA001071.
- Loeblich Jr., A.R., Tappan, H., 1987. Foraminiferal Genera and Their Classification.
- Van Nostrand Reinhold, New York. López-Urrutia, A., Martin, E.S., Harris, R.P., Irigoien, X., 2006. Scaling the metabolic balance of the oceans. Proc. Natl. Acad. Sci. 103, 8739-8744.
- Loubere, P., 1991. Deep-sea benthic foraminiferal assemblage response to a surface ocean productivity gradient: a test. Paleoceanography 6, 193-204.
- Loubere, P., 1994. Quantitative estimation of surface ocean productivity and bottom water oxygen concentration using benthic foraminifera. Paleoceanography 9, 723-737
- Loubere, P., 1998. The impact of seasonality on the benthos as reflected in the assemblages of deep-sea foraminifera. Deep-Sea Res. Part I 45, 409-432.
- Lyle, M., 2003. Neogene carbonate burial in the Pacific Ocean. Paleoceanography 18, 1059. https://doi.org/10.1029/2002PA000777.
- Lyle, M., Barron, J., Bralower, T.J., Huber, M., Lyle, A.O., Ravelo, A.C., Rea, D.K., Wilson, P.A., 2008. Pacific Ocean and cenozoic evolution of climate. Rev. Geophys. 46, RG2002. https://doi.org/10.1029/2005RG000190.
- Ma, Z., Gray, E., Thomas, E., Murphy, B., Zachos, J.C., Paytan, A., 2014. Carbon sequestration during the Paleocene-Eocene Thermal maximum by an efficient biological pump. Nat. Geosci. 7, 382–388. https://doi.org/10.1038/NGEO2139.
- Mackensen, A., Fütterer, D.K., Grobe, H., Schmiedl, G., 1993. Benthic foraminiferal assemblages from the eastern South Atlantic Polar Front region between 35° and 57: distribution, ecology and fossilization potential. Mar. Micropaleontol. 22, 33-39
- Mackensen, A., Globe, H., Kuhn, G., Fütterer, D.K., 1990. Benthic foraminiferal assemblages from the eastern Weddell Sea between 69 and 73: distribution, ecology and fossilization potential. Mar. Micropaleontol. 16, 241-283.
- Mackensen, A., Schmiedl, G., Harloff, J., Giese, M., 1995. Deep-sea foraminifera in the South Atlantic Ocean: ecology and assemblage generation. Micropaleontol. 41, 342 - 358.
- Martin, J.H., Knauer, G.A., Karl, D.M., Broenkow, W.W., 1987. VERTEX: carbon cycling in the northeast Pacific. Deep-Sea Res. Part I 34, 267-285.
- McGee, D., Marcantonio, F., Lynch-Stieglitz, J., 2007. Deglacial changes in dust flux in the eastern equatorial Pacific. Earth Planet. Sci. Lett. 257, 215-230.
- Messie, M., Chavez, F.P., 2013. Physical-biological synchrony in the global ocean associated with recent variability in the central and western equatorial Pacific. J. Geophys. Res., Oceans 118, 3782-3794.
- Meyers, G., Douguy, J.R., Reed, R.K., 1986. Evaporative cooling of the western equatorial Pacific by anomalous winds. Nature 323, 523-526.
- Murray, J., Young, J., Newton, J., Dunne, J., Chapin, T., Paul, B., McCarthy, J.J., 1996. Export flux of particulate organic carbon from the central equatorial Pacific determined using a combined drifting trap-²³⁴Th approach. Deep-Sea Res. Part II 43, 1095–1132. https://doi.org/10.1016/0967-0645(96)00036-7
- Nomaki, H., Heiz, P., Nakatsuka, T., Shimanaga, M., Ohkouchi, N., Ogawa, Kogure, K., Ikemoto, E., Kitazato, H., 2006. Different ingestion patterns of 13Clabeled bacteria and algae by deep-sea benthic foraminifera. Mar. Ecol. Prog. Ser. 310, 95-108.
- O'Connor, M.I., Piehler, M.F., Leech, D.M., Anton, A., Bruno, F., 2009. Warming and resource availability shift of food web structure and metabolism. PLoS Biol. 7, e1000178.
- Ohga, T., Kitazato, H., 1997. Seasonal changes in bathyal foraminiferal populations in response to the flux of organic matter (Sagami Bay, Japan). Terra. Nova 9, 33-37.

- Ohkushi, K., Thomas, E., Kawahata, H., 2000. Abyssal benthic foraminifera from the northwestern Pacific (Shatsky Rise) during the last 298 kyr. Mar. Micropaleontol. 38, 119–147.
- Oksanen, J., Blamchert, G.B., Kindt, R., Legendre, P., O'Hara, B., Simpson, G.L., Solymons, P., Stevens, M.H.H., Wagner, H., 2010. Vegan: Community Ecology Package. R package version v. 1. 17. 4. http://cran.r-project.org/web/packages/vegan/index.html.
- Passow, U., 2004. Switching perspectives: do mineral fluxes determine particulate organic carbon fluxes or vice versa? Geochem. Geophys. Geosyst. 5, Q04002. https://doi.org/10.1029/2003GC000670.
- Pena, L.P., Cacho, I., Ferretti, P., Hall, A., 2008. El-Niño—Southern Oscillation-like variability during glacial terminations and interlatitudinal teleconnections. Paleoceanography 23, PA3101. https://doi.org/10.1029/2008PA001620.
- R Development Core Team, 2010. R: a Language and Environments for Statistical Computing. R Foundation for Statistical Computing, Vienna, Austria. http://www.R-project.org.
- Rea, K.A., 1994. The paleoclimatic record provided by eolian deposition in the deep sea: the geologic history of wind. Rev. Geophys. 32, 159—195.
- Schmiedl, G., Mackensen, A., Müller, P.J., 1997. Recent benthic foraminifera from the eastern South Atlantic Ocean: dependence on food supply and water masses. Mar. Micropaleontol. 32, 249–287.
- Siddall, M., Hönish, B., Waelbroeck, C., Huybers, P., 2010. Changes in deep water temperature during mid-Pleistocene transiton and Quaternaty. Quat. Sci. Rev. 29, 170–181.
- Smart, C.W., King, S.C., Gooday, A.J., Murray, J.W., Thomas, E., 1994. A benthic foraminiferal proxy of pulsed organic matter paleofluxes. Mar. Micropaleontol. 23, 89–99.
- Smart, C.W., Thomas, E., Ramsay, A.T.S., 2007. Middle—late Miocene benthic foraminifera in a western equatorial Indian Ocean depth transect: paleoceanographic implications. Palaeogeogr. Palaeoclimatol. Palaeoecol. 247, 402–420.
- Sun, X., Corliss, B.H., Shower, W.J., 2006. The effect of primary productivity and seasonality on the distribution of deep-sea benthic foraminifera in the North Atlantic. Deep-Sea Res. Part I 53, 28–47.
- Takahashi, T., Sutherland, S.C., Wanninkhof, R., Sweeney, C., Feely, R.A., Chipman, D.W., Hales, B., Friederich, G., Chavez, F., Sabine, C., Watson, A., Bakker, D.C.E., Schuster, U., Metzl, N., Yoshikawa-Inoue, H., Ishii, M., Midorikawa, T., Nojiri, Y., Körtzinger, A., Steinhoff, T., Hoppema, M., Olfsson, J., Arnarson, T.S., Tilbrook, B., Johannessen, T., Olsen, A., Bellerby, R., Wong, C.S., Delille, B., Bates, N.R., de Baar, H.J.W., 2009. Climatological mean and decadal changes in surface ocean pCO₂, and net sea-air CO₂ flux over the global oceans. Deep-Sea Res. Part II 56, 554–577.
- Takata, H., Itaki, T., Ikehara, K., Khim, B.-K., 2018. Correlation between faunal transitions of benthic foraminifera and ballasting of particulate organic carbon by siliceous plankton during the Holocene off San-in district, southwestern Japan. Holocene 28, 444–454.
- Takata, H., Khim, B.-K., Yoo, C.M., Chi, S.-B., 2011. Shift in biotic response of abyssal benthic foraminifera since MIS 7 in the eastern equatorial Pacific Ocean. Geosci. J. 15, 417–422.
- Takata, H., Yoo, C.M., Kim, H.J., Khim, B.-K., 2016. Latitudinal difference on benthic foraminiferal fauna along ~131°W transect in the equatorial Pacific Ocean. Ocean Sci. J. 51, 655–663.

- Theyer, F., Mayer, L.A., Barron, J.A., Thomas, E., 1985. The equatorial pacific high-productivity belt: elements for a synthesis of deep sea drilling project leg 85 results. In: Mayer, L., Theyer, F., et al. (Eds.), Initial Reports of the Deep Sea Drilling Project, vol. 85, pp. 971–985.
- Thomas, E., 2007. Cenozoic mass extinctions in the deep sea: what perturbs the largest habitat on Earth? Geol. Soc. Am. Spec. Pap. 424, 1–23.
- Thomas, E., Booth, L., Maslin, M., Shackleton, N.J., 1995. Northeastern Atlantic benthic foraminifera during the last 45,000 years: productivity changes as seen from the bottom up. Paleoceanography 10, 545–562.
- Thomas, E., Gooday, A.J., 1996. Cenozoic deep-sea benthic foraminifers: tracer for changes in oceanic productivity. Geology 24, 355–358.
- Thomas, E., Turekian, K.K., Wei, K.-Y., 2000. Productivity control of fine particle transport to equatorial Pacific sediment. Glob. Biogeochem. Cycles 14, 945–955.
- Van Morkhoven, F.P.C.M., Berggren, W.A., Edwards, A.S., 1986. Cenozoic cosmopolitan deep-water benthic foraminifera. In: Bulletin des Centres de Recherches Exploration—Production Elf-Aquitaine, vol. 11.
- Waliser, D.E., Gautier, C., 1993. A satellite-derived climatology of the ITCZ. J. Clim. 6, 2162–2174.
- Webb, A.E., Leighton, L.R., 2011. Exploring the ecological dynamics of extinction. In: Laflamme, M., Schiffbauer, J.D., Dornbos, S.Q. (Eds.), Quantifying the Evolution of Earth Life, Topics in Geobiology, vol. 36. Springer, pp. 185–220.
- Webb, A.E., Leighton, L.R., Schellenberg, S.A., Landau, E.A., Thomas, E., 2009. Impact of the Paleocene-Eocene thermal maximum on deep-ocean microbenthic community structure: using rank-abundance curves to quantify paleoecological response. Geology 37, 783–786.
- Willett, C.S., Leben, R.R., Lavin, M.F., 2006. Eddies and tropical instability waves in the eastern tropical pacific: a review. Prog. Oceanogr. 69, 218–238.
- Yamazaki, T., 2012. Paleoposition of the Intertropical Convergence Zone in the eastern Equatorial Pacific inferred from glacial—interglacial changes in terrigenous and biogenic magnetic mineral fractions. Geology 40, 151–154.
- Yasuhara, M., Cronin, T.M., 2008. Climatic influences on deep-sea ostracode (CRUSTACEA) diversity for the last three million years. Ecology 89, S53—S65.
- Yasuhara, M., Cronin, T.M., deMenocal, P.B., Okahashi, H., Linsley, B.K., 2008. Abrupt climate change and collapse of deep-sea ecosystems. Proc. Natl. Acad. Sci. 105, 1556—1560.
- Yasuhara, M., Hunt, G., Cronin, T.M., Hokanishi, N., Kawahata, H., Tsujimoto, A., Ishitake, M., 2012. Climate forcing of quaternary Deep-sea benthic communities in the north Pacific Ocean. Paleobiology 38, 162–179.
- Yasuhara, M., Hunt, G., Cronin, T.M., Okahashi, H., 2009. Temporal latitudinal-gradient dynamics and tropical instability of deep-sea species diversity. Proc. Natl. Acad. Sci. 106, 21717—21720.
- Yasuhara, M., Tittensor, D.P., Hillebrand, H., Worm, B., 2017. Combining marine macroecology and palaeoecology in understanding biodiversity: microfossils as a model. Biol. Rev. 92, 199–215.
- Yu, P.-S., Kienast, M., Chen, M.-T., Cacho, I., Flores, J.A., 2017. Surface hydrographic and water mass variability in the eastern equatorial Pacific during interglaciallike Marine Isotope Stage 14. Quat. Internl. 436, 45–56.
- Zhang, J., Wang, P., Li, Q., Cheng, X., Jin, H., Zhang, S., 2007. Western equatorial Pacific productivity and carbonate dissolution over the last 550 kyr: foraminiferal and nannofossil evidence from ODP Hole 807A. Mar. Micropaleonol. 64, 121–140.